ELECTROMAGNETIC METAMATERIALS: TRANSMISSION LINE THEORY AND MICROWAVE APPLICATIONS

The Engineering Approach

CHRISTOPHE CALOZ
École Polytechnique de Montréal

TATSUO ITOH
University of California at Los Angeles

A JOHN WILEY & SONS, INC., PUBLICATION

Published by John Wiley & Sons, Inc., Hoboken, New Jersey.
Published simultaneously in Canada.

Library of Congress Cataloging-in-Publication Data:

Caloz, Christophe, 1969-
Electromagnetic metamaterials : transmission line theory and microwave applications : the engineering approach / Christophe Caloz, Tatsuo Itoh.
p.cm.
"Wiley-Interscience publication."
Includes bibliographical references and index.
ISBN-10: 0-471-66985-7 (alk.paper)
ISBN-13: 978-0-471-66985-2 (alk.paper)
1. Magnetic materials. 2. Nanostructured materials. 3. Microwave transmission lines. I. Itoh, Tatsuo. II. Title.

TK454.4.M3C36 2006
620.1′18—dc22

2005048976

Printed in the United States of America.

10 9 8 7 6 5 4 3 2 1

To Dominique, Maxime, and Raphaël
Christophe

CONTENTS

PREFACE

This book is essentially the fruit of a research work carried out at University of California, Los Angeles (UCLA), from 2002 to 2004 in the context of a Multidisciplinary University Research Initiative (MURI) program. The main participants in this program, in addition to the authors, were John Pendry (Imperial College), David Smith (formerly University of California, San Diego (UCSD), now Duke University), Sheldon Schultz (UCSD), Xiang Zhang (formerly UCLA, now University of California, Berkeley), Gang Chen (formerly UCLA, now Massachusetts Institute of Technology (MIT)), John Joannopoulos (MIT) and Eli Yablonovitch (UCLA).

During these years of infancy for metamaterials (MTMs), which emerged from the first experimental demonstration of a left-handed (LH) structure in 2000, the vast majority of the groups involved in research on MTMs had been focusing on investigating from a physics point of view the fundamental properties of LH media predicted by Veselago in 1967. Not following this trend, the authors adopted an engineering approach, based on a generalized transmission line (TL) theory, with systematic emphasis on developing practical applications, exhibiting unprecedented features in terms of performances or functionalities. This effort resulted in the elaboration of the powerful composite right/left-handed (CRLH) MTM concept, which led to a suite of novel guided-wave, radiated-wave, and refracted-wave devices and structures.

This book presents electromagnetic MTMs and their applications in the general framework of CRLH TL MTMs. Chapter 1 introduces MTMs from a historical perspective and points out their novelty compared with conventional periodic backward-wave media. Chapter 2 exposes the fundamentals of ideal[1]

[1]"Ideal" designates here perfectly homogeneous and isotropic volumic (left-handedness along the three directions of space) materials.

LH MTMs, including the antiparallelism existing between phase/group velocities, the frequency dispersion required from entropy conditions, the modified boundary conditions, the modified Fresnel coefficients, the reversal of classical phenomena [Doppler effect, Vavilov-Čerenkov radiation, Snell's law (negative refractive index, NRI), Goos-Hänchen effect, lenses convergence/divergence], and focusing by a flat "lens" and subwavelength diffraction. Chapter 3 establishes the foundations of CRLH structures, in three progressive steps: ideal TL, LC network, and real distributed structure. Chapter 4 extends theses foundations to the two-dimensional (2D) case, develops a transmission matrix method (TMM) and a transmission line method (TLM) techniques to address the problem of finite-size 2D MTMs excited by arbitrary sources, illustrates by TLM simulations a few NRI effects occurring in 2D MTMs (backward-wave propagation, negative refraction by a RH-LH interface, a LH slab, a LH prism, inner reflection of Gaussian beams in a LH prism, and a LH "perfectly absorbing reflector"), and describes real distributed implementations of 2D MTMs. Chapter 5 presents guided-wave applications of CRLH TL MTMs, including dual-band components, enhanced-bandwidth components, a super-compact multilayer "vertical" structure, tight edge-coupled directional couplers, and negative/zeroth-order resonators. Chapter 6 presents radiated-wave applications of CRLH TL MTMs, including 1D or 2D frequency-scanned and electronically scanned leaky-wave antennas and reflecto-directive systems. Finally, future challenges and prospects of MTMs, including homogenized MTMs, quasi-optical NRI lenses, 3D isotropic LH structures, optical MTMs, magnetless magnetic MTMs, surface plasmonic MTMs, MTMs antenna radomes and frequency selective surfaces, nonlinear, and active MTMs, are discussed in Chapter 7.

It is hoped that the engineering approach of MTMs presented in this book will pave the way for a novel generation of microwave and photonic devices and structures.

C. CALOZ AND T. ITOH

Montéal, Québec, and Los Angeles, California

ACKNOWLEDGMENTS

Many researchers have contributed to the realization of this book.

The authors thank all the master's and Ph.D. students of UCLA who have been involved in this work: Anthony Lai, Sungjoon Lim, I-Hsiang Lin, Catherine Allen, Lei Liu, Simon Otto, Chen-Jung Lee, and Marc de Vincentis.

In addition, the authors express their gratitude to several visiting scholars of UCLA, who had various degrees of participation in this research, including Hiroshi Okabe (Hitachi Central Research Laboratory), Yasushi Horii (Kansai University), Taisuke Iwai (Fujitsu's Research Labs), and Dal Ahn (Soonchunhyang University). Special thanks are addressed to Atsushi Sanada (Yamagushi University), who played a major role in the development of several concepts and applications presented in the book.

Finally, very special thanks are addressed to Wolfgang Hoefer, University of Victoria, British Columbia, who kindly accepted to contribute to this work by authoring two sections in Chapter 4 on the transmission line method (TLM) analysis of 2D metamaterials.

This work was part of the MURI program "Scalable and Reconfigurable Electromagnetic Metamaterials and Devices." It was supported by the Department of Defense (program N00014-01-1-0803) and monitored by the U.S. Office of Naval Research.

C. C. AND T. I.

ACRONYMS

ATR	Attenuated total reflection
BCs	Boundary conditions
BE	Backfire-to-endfire
BWO	Backward-wave oscillator
BZ	Brillouin zone
CRLH	Composite right/left-handed
CLC	Coupled-line coupler
DB	Dual-band
DPDS	Dual-passband dual-stopband
FDTD	Finite-difference time domain
FEM	Finite-element method
FSS	Frequency selective surface
GVD	Group velocity dispersion
IC	Impedance coupling or coupler
LH	Left-handed
LTCC	Low-temperature cofired ceramics
LW	Leaky-wave
MIM	Metal-insulator-metal
MTM	Metamaterial
MLV	Multilayered vertical
MoM	Method of moments
MRI	Magnetic resonance imaging
MSBVW	Magnetostatic backward volume wave
NRI	Negative refractive index
OPL	Optical path length

PC	Phase coupling or coupler
PCB	Printed circuit board
PBCs	Periodic boundary conditions
PBG	Photonic band-gap
PPWG	Parallel-plate waveguide
PLH	Purely left-handed
PRH	Purely right-handed
QH	Quadrature hybrid
RH	Right-handed
RCS	Radar cross section
RDS	Reflecto-directive system
RRC	Rat-race coupler
SHPM	Subharmonically pumped mixer
SP	Surface plasmon
SPM	Self-phase modulation
SRR	Split-ring resonator
TE	Transverse electric
TEM	Transverse electric-magnetic
TH	Thin-wire
TL	Transmission line
TLM	Transmission line method
TM	Transverse magnetic
TMA	Transfer matrix algorithm
TMM	Transmission matrix method
TWT	Traveling-Wave Tube
UWB	Ultra wideband
ZOR	Zeroth-order resonator

1

INTRODUCTION

Chapter 1 introduces electromagnetic metamaterials (MTMs) and left-handed (LH) MTMs from a general prospect. Section 1.1 defines them. Section 1.2 presents the theoretical speculation by Viktor Veselago on the existence of "substances with simultaneously negative ε and μ" in 1967, which is at the origin of all research on LH MTMs. Section 1.3 describes the first experimental demonstration of left-handedness in 2000 by Smith et al., and Section 1.4 lists a number of further numerical, theoretical, and experimental confirmations of the fundamental properties of LH structures. The difference between "conventional" backward waves, known for many decades, and LH waves, as well as the essential novelty of LH MTMs, are explained in Section 1.5. Section 1.6 discusses the different terminologies used in the literature to designate LH MTMs. Next, Section 1.7 introduces the transmission line (TL) approach of LH MTMs, which has constituted a decisive step toward microwave applications, and Section 1.8 presents, in a concise manner, the generalized composite right/left-handed (CRLH) concept upon which the whole book is based. Finally, Section 1.9 points out the essential difference existing between photonic crystals or photonic band-gap (PBG) structures, more conventionally simply called "periodic structures", and MTMs.

1.1 DEFINITION OF METAMATERIALS (MTMs) AND LEFT-HANDED (LH) MTMs

Electromagnetic metamaterials (MTMs) are broadly defined as *artificial effectively homogeneous electromagnetic structures with unusual properties not readily*

Electromagnetic Metamaterials: Transmission Line Theory and Microwave Applications,
By Christophe Caloz and Tatsuo Itoh

available in nature. An *effectively homogeneous* structure is a structure whose *structural average cell size* p is *much smaller than the guided wavelength* λ_g. Therefore, this average cell size should be at least smaller than a quarter of wavelength, $p < \lambda_g/4$. We will refer to the condition $p = \lambda_g/4$ as the *effective-homogeneity limit* or *effective-homogeneity condition*[1], to ensure that *refractive phenomena* will dominate over *scattering/diffraction* phenomena when a wave propagates inside the MTM medium. If the condition of effective-homogeneity is satisfied, the structure behaves as a real material in the sense that electromagnetic waves are essentially *myopic to the lattice* and only probe the average, or effective, macroscopic and well-defined *constitutive parameters, which depend on the nature of the unit cell*; the structure is thus *electromagnetically uniform* along the direction of propagation. The constitutive parameters are the permittivity ε and the permeability μ, which are related to the refractive index n by

$$n = \pm\sqrt{\varepsilon_r \mu_r}, \tag{1.1}$$

where ε_r and μ_r are the relative permittivity and permeability related to the free space permittivity and permeability by $\varepsilon_0 = \varepsilon/\varepsilon_r = 8.854 \cdot 10^{-12}$ and $\mu_0 = \mu/\mu_r = 4\pi \cdot 10^{-7}$, respectively. In (1.1), sign $\pm$ for the double-valued square root function has been a priori admitted for generality.

The four possible sign combinations in the pair (ε, μ) are $(+,+)$, $(+,-)$, $(-,+)$, and $(-,-)$, as illustrated in the $\varepsilon - \mu$ diagram of Fig 1.1. Whereas the first three combinations are well known in conventional materials, the last one $[(-,-)]$, with *simultaneously negative permittivity and permeability*, corresponds to the new class of left-handed (LH) materials.[2] LH materials, as a consequence of their double negative parameters, are characterized by antiparallel phase and group velocities, or negative refractive index (NRI) [negative sign in Eq. (1.1)], as will be shown in Chapter 2.

LH structures are clearly MTMs, according to the definition given above, since they are artificial (fabricated by human hands), effectively homogeneous ($p < \lambda_g/4$), and exhibit highly unusual properties ($\varepsilon_r, \mu_r < 0$). It should be noted that, although the term MTM has been used most often in reference to LH structures in the literature, MTMs may encompass a much broader range of

[1]This limit corresponds to a rule of thumb effectiveness condition. Microwave engineers often use the limit $p = \lambda_g/4$, where p is the size of the component considered, to distinguish lumped components ($p < \lambda_g/4$) from quasi-lumped components ($\lambda_g/4 < p < \lambda_g/2$) and distributed components ($p > \lambda_g/2$) [1]. In the lumped case, the phase variation of the signal from the input to the output of the component is negligible, and the component may therefore be considered as a localized (sizeless) element. In contrast, in the distributed case, phase variation along the component cannot be ignored, and the component must consequently be considered as a transmission line section. MTMs are thus "distributed structures constituted of lumped elements."

[2]It should be noted that thin ferrimagnetic films biased in the plane of the film support magnetostatic backward volume wave (MSBVW) in the direction of bias, which may be seen as a LH phenomenon (Section 2.1) in a *real* material. However, this phenomenon is strictly dependent on the thin slab shape of the film and could not exist per se in a bulk ferrite and is therefore not an isotropic LH effect.

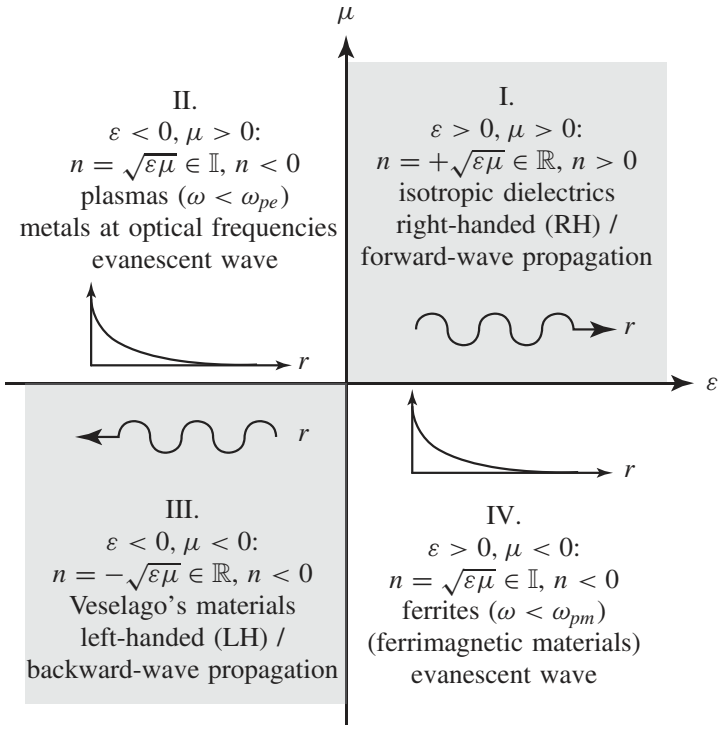

Fig. 1.1. Permittivity-permeability ($\varepsilon - \mu$) and refractive index (n) diagram. The time dependence $e^{+j\omega t}$, associated with the *outgoing* wave function $e^{-j\beta r}$ or *incoming* wave function $e^{+j\beta r}$, where β is the propagation constant, $\beta = nk_0$ ($k_0 = \omega/c$: free space wavenumber, ω: angular frequency, c: speed of light), is assumed. The angular frequencies ω_{pe} and ω_{pm} represent the electric and magnetic plasma frequencies, respectively. $\mathbb{R}$, purely real. $\mathbb{I}$, purely imaginary.

structures.[3] However, LH structures have been by far the most popular of the MTMs, due to their exceptional property of negative refractive index (Chapter 2). This book mainly deals with this class of MTMs and, more precisely, with composite right/left-handed (CRLH) MTMs (Section 1.8), which constitute a generalization of LH MTMs.

1.2 THEORETICAL SPECULATION BY VIKTOR VESELAGO

The history of MTMs started in 1967 with the visionary speculation on the existence of *"substances with simultaneously negative values of ε and μ"* (fourth

[3]Examples are MTMs with only one of the two constitutive parameters negative, anisotropic MTMs, or any type of functional effective engineered structure. In addition, many existing materials obtained by novel nanotechnology and chemistry processes may be regarded as MTMs.

quadrant in Fig 1.1) by the Russian physicist Viktor Veselago [3].[4] In his paper, Veselago called these "substances" LH to express the fact that they would allow the propagation of electromagnetic waves with the electric field, the magnetic field, and the phase constant vectors building a left-handed triad, compared with conventional materials where this triad is known to be *right-handed* (Section 2.1).

Several fundamental phenomena occurring in or in association with LH media were predicted by Veselago:

1. Necessary frequency dispersion of the constitutive parameters (Section 2.2).
2. Reversal of Doppler effect (Section 2.4).
3. Reversal of Vavilov-Cerenkov radiation (Section 2.5).
4. Reversal of the boundary conditions relating the normal components of the electric and magnetic fields at the interface between a conventional/right-handed (RH) medium and a LH medium (Section 2.3).
5. Reversal of Snell's law (Section 2.6).
6. Subsequent negative refraction at the interface between a RH medium and a LH medium (Section 2.6).
7. Transformation of a point source into a point image by a LH slab (Section 2.6).
8. Interchange of convergence and divergence effects in convex and concave lenses, respectively, when the lens is made LH (Section 2.6).
9. Plasmonic expressions of the constitutive parameters in resonant-type LH media (Section 1.3).

Veselago concluded his paper by discussing potential *real* (natural) "substances" that could exhibit left-handedness. He suggested that "gyrotropic substances possessing plasma and magnetic properties" ("pure ferromagnetic metals or semiconductors"), "in which both ε and μ are tensors" (anisotropic structures), could possibly be LH.[5] However, he recognized, "Unfortunately, . . . , we do not know of even a single substance which could be isotropic and have $\mu < 0$," thereby pointing out how difficult it seemed to realize a practical LH structure. No LH material was indeed discovered at that time.

1.3 EXPERIMENTAL DEMONSTRATION OF LEFT-HANDEDNESS

After Veselago's paper, more than 30 years elapsed until the first LH material was conceived and demonstrated experimentally. This LH material was not a natural substance, as expected by Veselago, but an *artificial* effectively homogeneous

[4]This paper was originally published in Russian in 1967 and then translated into English in 1968. In this translation, the date of 1964 is indicated by mistake as the publication year of the original Russian version.

[5]This is indeed the case, in a restricted sense, of ferrite films supporting MSBVWs, as pointed out in note 2.

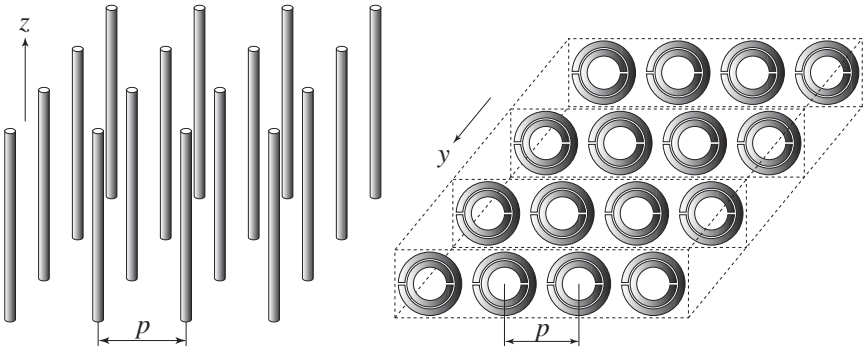

Fig. 1.2. First negative-ε/positive-μ and positive-ε/negative-μ MTM ($p \ll \lambda_g$), constituted only by standard metals and dielectrics, proposed by Pendry. (a) Thin-wire (TW) structure exhibiting negative-ε/positive-μ if $\mathbf{E} \| z$ [6]. (b) Split-ring resonator (SRR) structure exhibiting positive-ε/negative-μ if $\mathbf{H} \perp y$ [7].

structure (i.e., a MTM), which was proposed by Smith and colleagues at University of California, San Diego (UCSD) [4].[6] This structure was inspired by the pioneering works of Pendry at Imperial College, London. Pendry introduced the *plasmonic-type* negative-ε/positive-μ and positive-ε/negative-μ structures shown in Fig 1.2, which can be designed to have their *plasmonic frequency in the microwave range*.[7] Both of these structures have an average cell size p much smaller than the guided wavelength λ_g ($p \ll \lambda_g$) and are therefore effectively homogeneous structures, or MTMs.

The negative-ε/positive-μ MTM is the *metal thin-wire (TW)* structure shown in Fig 1.2(a). If the excitation electric field $\mathbf{E}$ is parallel to the axis of the wires ($\mathbf{E} \| z$), so as to induce a current along them and generate equivalent electric dipole moments,[8] this MTM exhibits a plasmonic-type permittivity frequency function of the form [5, 6]

$$\varepsilon_r(\omega) = 1 - \frac{\omega_{pe}^2}{\omega^2 + j\omega\zeta} = 1 - \frac{\omega_{pe}^2}{\omega^2 + \zeta^2} + j\frac{\zeta\omega_{pe}^2}{\omega(\omega^2 + \zeta^2)}, \tag{1.2}$$

where $\omega_{pe} = \sqrt{2\pi c^2/[p^2 \ln(p/a)]}$ (c: speed of light, a: radius of the wires) is the *electric plasma frequency*, tunable in the GHz range, and $\zeta = \varepsilon_0(p\omega_{pe}/a)^2/\pi\sigma$

[6]The fact that this first LH MTM was artificial, as all the other LH MTMs known to date!, does not at all exclude that natural substances exhibiting left-handedness could be discovered some day. Because left-handedness is allowed by fundamental physics laws in artificial structures, there is no reason why it would not be also possible in natural substances.

[7]This is distinct from conventional gas and metal plasmas, which have their plasma frequency far above the microwave range, preventing negative ε at microwave frequencies.

[8]If the electric field $\mathbf{E}$ is perfectly parallel to the axis of the wires (z), a maximum of effect is obtained. If it is exactly perpendicular to the wires, we have a situation of cross polarization, where no effect is produced. In the intermediate situation where the electric field is oblique with respect to the wires, a reduced effect occurs, decreasing as the angle with the wires increases.

(σ: conductivity of the metal) is a damping factor due to metal losses. It clearly appears in this formula that

$$\mathrm{Re}(\varepsilon_r) < 0, \quad \text{for} \quad \omega^2 < \omega_{pe}^2 - \zeta^2, \tag{1.3a}$$

which reduces if $\zeta = 0$ to

$$\varepsilon_r < 0, \quad \text{for} \quad \omega < \omega_{pe}. \tag{1.3b}$$

On the other hand, permeability is simply $\mu = \mu_0$, since no magnetic material is present and no magnetic dipole moment is generated. It should be noted that the wires are assumed to be much longer than wavelength (theoretically infinite), which means that the wires are excited at frequencies situated far below their first resonance.

The positive-ε/negative-μ MTM is the *metal split-ring resonator (SRR)* structure[9] shown in Fig 1.2(b). If the excitation magnetic field $\mathbf{H}$ is perpendicular to the plane of the rings ($\mathbf{H} \perp y$), so as to induce resonating currents in the loop and generate equivalent *magnetic dipole moments*,[10] this MTM exhibits a plasmonic-type permeability frequency function of the form [7]

$$\begin{aligned} \mu_r(\omega) &= 1 - \frac{F\omega^2}{\omega^2 - \omega_{0m}^2 + j\omega\zeta} \\ &= 1 - \frac{F\omega^2(\omega^2 - \omega_{0m}^2)}{(\omega^2 - \omega_{0m}^2)^2 + (\omega\zeta)^2} + j\frac{F\omega^2\zeta}{(\omega^2 - \omega_{0m}^2)^2 + (\omega\zeta)^2}, \end{aligned} \tag{1.4}$$

where $F = \pi(a/p)^2$ (a: inner radius of the smaller ring), $\omega_{0m} = c\sqrt{\frac{3p}{\pi \ln(2wa^3/\delta)}}$ (w: width of the rings, δ: radial spacing between the rings) is a magnetic resonance frequency, tunable in the GHz range, and $\zeta = 2pR'/a\mu_0$ (R': metal resistance per unit length) is the damping factor due to metal losses. It should be noted that the SRR structure has a magnetic response despite the fact that it does not include magnetic conducting materials due to the presence of artificial magnetic dipole moments provided by the ring resonators. Eq. (1.4) reveals that a frequency range can exist in which $\mathrm{Re}(\mu_r) < 0$ in general ($\zeta \neq 0$). In the loss-less case ($\zeta \neq 0$), it appears that

$$\mu_r < 0, \quad \text{for} \quad \omega_{0m} < \omega < \frac{\omega_{0m}}{\sqrt{1-F}} = \omega_{pm}, \tag{1.5}$$

where ω_{pm} is called the *magnetic plasma frequency*. An essential difference between the plasmonic expressions of ε and μ is that the latter is of *resonant*

[9]One single ring in the unit cell produces qualitatively identical effects, but the magnetic activity, effective permeability and bandwidth, is enhanced by the presence of a second ring due to larger overall current and slightly different overlapping resonances.

[10]A remark analogous to that of note 8 holds here under the substitutions $\mathbf{E} \to \mathbf{H}$ and $z \to y$.

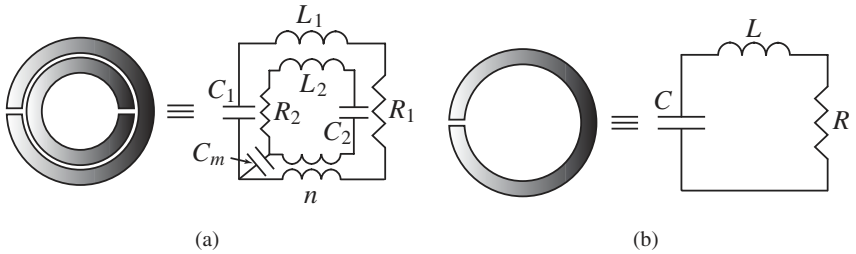

Fig. 1.3. Equivalent circuit model of SRRs. (a) Double SRR configuration (e.g., [7]). (b) Single SRR configuration.

nature [$\mu(\omega = \omega_{0m}) = \infty$], whereas the former is a nonresonant expression. The resonance of the structure is due to the resonance of its SRRs, given in [7] by $\omega_{0m}^2 = 3pc^2/[\pi \ln(2w/\delta]a^3)$ (p: period, $c = 1/\sqrt{\varepsilon_0\mu_0}$: speed of light, w: width of the rings, δ: spacing between the rings).

The equivalent circuit of a SRR is shown in Fig 1.3 [8]. In the double ring configuration [Fig 1.3(a)], capacitive coupling and inductive coupling between the larger and smaller rings are modeled by a coupling capacitance (C_m) and by a transformer (transforming ratio n), respectively. In the single ring configuration [Fig 1.3(b)], the circuit model is that of the simplest RLC resonator with resonant frequency $\omega_0 = 1/\sqrt{LC}$. The double SRR is essentially equivalent to the single SRR if mutual coupling is weak, because the dimensions of the two rings are very close to each other, so that $L_1 \approx L_2 \approx L$ and $C_1 \approx C_2 \approx C$, resulting in a combined resonance frequency close to that of the single SRR with same dimensions but with a larger magnetic moment due to higher current density.

In [4], Smith et al. combined the TW and SRR structures of Pendry into the composite structure shown in Fig 1.4(a), which represented the first experimental LH MTM prototype. The arguments in [4] consisted of the following: 1) designing a TW structure and a SRR structure with overlapping frequency ranges of negative permittivity and permeability; 2) combining the two structures into a composite TW-SRR structure, which is shown in Fig 1.4(a); and 3) launching an electromagnetic wave $e^{-j\beta r}$ through the structure and concluding from a fact that a passband (or maximum transmission coefficient, experimentally) appears in the frequency range of interest proves that the constitutive parameters are simultaneously negative in this range on the basis of the fact that $\beta = nk_0 = \pm\sqrt{\varepsilon_r\mu_r}$ has to be real in a passband.

Although the arguments of [4] were questionable, because it ignored the fact that coupling interactions between the two constituent structures could yield properties totally different from the superposition of the properties of each structure taken separately,[11] a vivid experimental demonstration of the LH nature of the TW-SRR was provided in [10]. In this paper, the TW-SRR structure of Fig 1.4(b)

[11]In fact, this structure was really "working" only due to the judicious position of the wires in the symmetry center of the rings, which canceled interactions between the two structures due to induced

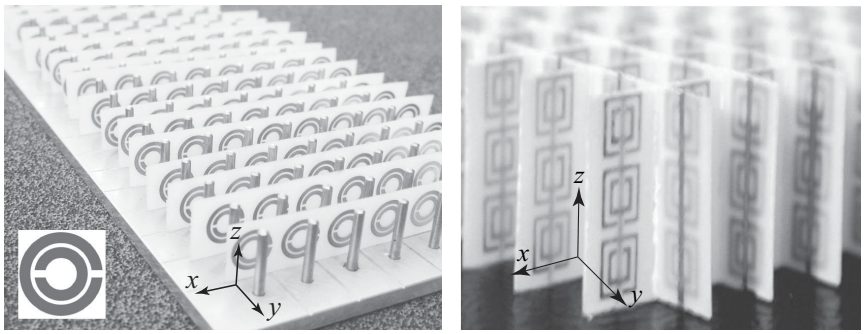

(a) (b)

Fig. 1.4. First experimental LH structures, constituted of TWs and SRRs, introduced by the team of UCSD. (a) Monodimensionally LH structure of [4]. (b) Bidimensionally LH structure of [10].

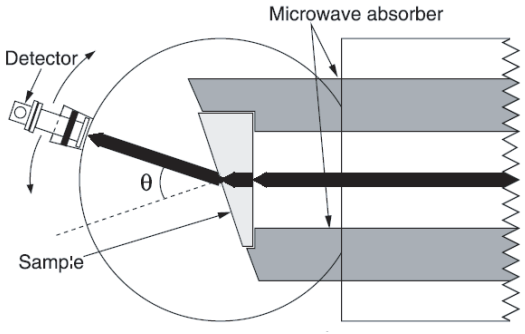

Fig. 1.5. Experimental setup used in [10] for the demonstration of left-handedness of the TW-SRR structure of Fig 1.4(b) at around 5 GHz. "The sample and the microwave absorber were placed between top and bottom parallel, circular aluminum plates spaced 1.2 cm apart. The radius of the circular plates was 15 cm. The black arrows represent the microwave beam as would be refracted by a positive index sample. The detector was rotated around the circumference of the circle in 1.5° steps, and the transmitted power spectrum was measured as a function of angle, θ, from the interface normal. The detector was a waveguide to coaxial adapter attached to a standard X-band waveguide, whose opening was 2.3 cm in the plane of the circular plates. θ as shown is positive in this figure." From [10], © Science; reprinted with permission.

was cut into a wedge-shaped piece of MTM and inserted into the experimental apparatus depicted in Fig 1.5. Left-handedness of the TW-SRR structure was evidenced by the fact that a maximum of the transmission coefficient was measured in the negative angle (below the normal in the figure) with respect to the

currents with opposite signs in the SRRs and TWs [9]. Note that there an other possible symmetry location for the TWs is in the midplanes between the SRRs.

interface of the wedge, whereas a maximum in the positive angle (above the normal) was measured, as expected, when the wedge was replaced by a regular piece of teflon with identical shape. The result reported was in qualitative and quantitative agreement with *Snell's law*, which reads

$$k_1 \sin\theta_1 = k_2 \sin\theta_2, \tag{1.6a}$$

or, if the two media are isotropic (so that $k_1 = n_1 k_0$ and $k_2 = n_2 k_0$),

$$n_1 \sin\theta_1 = n_2 \sin\theta_2, \tag{1.6b}$$

where k_i, n_i, and θ_i represent the wavenumber, refractive index, and angle of the ray from the normal to the interface, respectively, in each of the two media considered ($i = 1, \ldots, 2$).

The MTMs described here are *anisotropic*[12] and characterized by uniaxial permittivity and permeability tensors

$$[\varepsilon] = \begin{bmatrix} \varepsilon_{xx} & 0 & 0 \\ 0 & \varepsilon_{yy} & 0 \\ 0 & 0 & \varepsilon_{zz} \end{bmatrix}, \tag{1.7a}$$

$$[\mu] = \begin{bmatrix} \mu_{xx} & 0 & 0 \\ 0 & \mu_{yy} & 0 \\ 0 & 0 & \mu_{zz} \end{bmatrix}. \tag{1.7b}$$

The structure shown in Fig 1.4(a) is monodimensionally LH, since only one direction is allowed for the doublet (**E**, **H**); we have $\varepsilon_{xx}(\omega < \omega_{pe}) < 0$ and $\varepsilon_{yy} = \varepsilon_{zz} > 0$, $\mu_{xx}(\omega_{0m} < \omega < \omega_{pm}) < 0$ and $\mu_{yy} = \mu_{zz} > 0$. The structure shown in Fig 1.4(b) is bidimensionally LH because, although **E** has to be directed along the axis of the wires, two directions are possible for **H**; then $[\varepsilon]$ is unchanged, but $\mu_{xx}, \mu_{yy} < 0$ for $\omega_{0m} < \omega < \omega_{pm}$ and $\mu_{zz} > 0$.

1.4 FURTHER NUMERICAL AND EXPERIMENTAL CONFIRMATIONS

In the few years after the first experimental demonstration of a LH structure by Smith et al., a large number of both theoretical and experimental reports confirmed the existence and main properties of LH materials predicted by Veselago.[13]

Characterization of the *TW-SRR LH structures* in terms of constitutive parameter functions similar to Eqs. (1.2) and (1.4) was provided by Smith et al. in [12], [13], and [14] and was then abundantly rediscussed and refined by various

[12]It is worth noting that various spatial filtering effects may be obtained from this anisotropic MTM [11].

[13]In 2002, some controversies temporarily cast doubt on these novel concepts [15, 16, 17]. However, these controversies were quickly shown to be based on physics misconceptions (e.g., [35]).

TABLE 1.1. Verification of Main Properties and Fundamental Physics of LH MTMs by Different Approaches and Different Groups.

Type of Investigation	References
Numerical FDTD	Ziolkowski et al. [27, 28]
Numerical FEM	Caloz et al. [29]
Numerical TMA	Markŏs et al. [20, 21]
Numerical TLM	So and Hoefer [30, 31]
Theoretical EM	Lindell et al. [32], Kong et al. [33, 34], Smith et al. [35], McCall et al. [36]
Experimental (bulk) TW-SRR	Shelby et al. [10], Greegor et al. [22], Ziolkowski [26], Marqués et al. [25]
Theoretical TL	Eleftheriades et al. [37, 38], Caloz and Itoh [39, 40], Oliner [41, 42]
Experimental (planar) TL	Iyer et al. [43], Caloz and Itoh [40], Sanada et al. [44]

groups, all confirming the LH nature of these structures (e.g., [18, 19, 20, 21, 22, 23, 24, 25, 26]).

Table 1.1 presents a list of key reports verifying, by different approaches, the main properties and fundamental physics of LH MTMs. The main *numerical methods* used are finite-difference time-domain (FDTD), finite-elements method (FEM), transfer matrix algorithm (TAM), and transmission line method (TLM). The *theoretical* verifications are subdivided into fundamental electromagnetic (EM) theory and transmission line (TL) theory approaches. *Experimental* demonstrations are provided both in TW-SRR bulk structures and planar TL-type structures.

1.5 "CONVENTIONAL" BACKWARD WAVES AND NOVELTY OF LH MTMs

Propagation of waves with antiparallel phase and group velocity is not a new phenomenon. It has been known for many years in the physics and microwave communities in various contexts. Back in the late 1940s, Brillouin and Pierce utilized the series-capacitance/shunt-inductance equivalent circuit model shown in Fig 1.6, which constitutes the starting point of the CRLH TL theory and applications presented in this book, to describe such antiparallel phase/group velocities propagation, and used the term *backward waves* to designate the corresponding waves [45, 46].[14] For Brillouin, backward waves referred to negative space

[14]We may also add Malyuzhinets, who also used the same LC model, after Brillouin and Pierce, in the description of the radiation condition in backward-wave media [47].

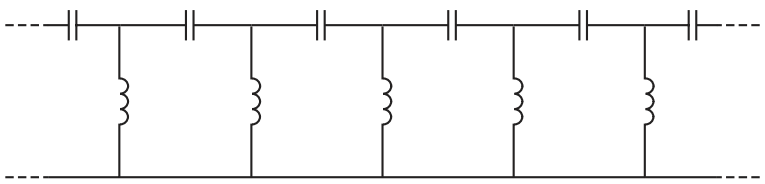

Fig. 1.6. Equivalent circuit model for a line supporting a backward wave.

harmonics contributing in the Fourier series expansion of fields in periodic structures, while for Pierce and colleagues backward waves were related to the phenomenon of backward amplification in traveling wave tubes (TWT).[15] Several classical textbooks describing backward waves are available [48, 49].

However, in both Brillouin's and Pierce's cases, and it seems in all other known occurrences of backward-wave phenomena in the literature, perhaps with the exception of magnetostatic backward volume waves (MSBVWs) [2], backward waves are associated with either *space harmonics* or *higher-order modes* of the structures. Therefore, these structures have a period typically of the order of one-half the guided wavelength ($p \approx \lambda_g/2$), or multiple of half the guided wavelength for higher space harmonics or higher modes ($p \approx n\lambda_g/2$). Consequently, propagation along these conventional backward-wave structures are dominated by diffraction/scattering phenomena, so that they cannot be characterized by constitutive parameters ε and μ.[16] Extended to 2D or 3D, if possible, they would not exhibit the electromagnetic behavior of real materials, as for instance refractive properties obeying to simple laws such as Snell's law.

In contrast, LH MTMs are operating in their *fundamental mode* (effectively homogeneous), where $p \ll \lambda_g$, so that effective macroscopic ε and μ can be rigorously defined. They are thus behaving as "real" materials. In fact, as long as $p < \lambda_g/4$, the difference between a LH MTM and a natural dielectric material (such as glass or Teflon) is only *quantitative*. In the case of the natural dielectric material, the structural units inducing a given permittivity value are the constitutive molecules, which are of the order of the Angström, while in the case of current LH materials, the structural units are of the order of the centimeter in the microwave range; thus, in the microwave $L - X$ bands, the electrical size of the structural unit in the former case is of the order of $p/\lambda_g \approx 10^{-9}$ while it is of the order of $p/\lambda_g \approx 10^{-1} - 10^{-2}$ in the latter case. But *qualitatively*, similar refractive phenomena occur in LH MTMs as in conventional dielectrics. This is the point at which the fundamental originality of LH-MTMs lies: LH-MTMs represent artificial structures behaving in the same manner as conventional bulk dielectrics, hence the term "material" in meta-materials, but with negative constitutive parameters. The subsequent and fundamental originality of LH MTMs

[15]Backward-wave oscillators (BWOs), which are realized by coupling some of the output power of a TWT back into its input, also exhibit backward-wave properties reminiscent to those of LH structures.

[16]In this regard, they can be termed "structures" but not artificial "materials" or MTMs.

is that, due to their effective homogeneity, they can be extended to 2D and potentially 3D isotropic MTMs.

1.6 TERMINOLOGY

To date, there is no consensus regarding the terminology designating MTMs with simultaneously negative permittivity and permeability. Several equivalent terminologies have been used, each of which presenting advantages and disadvantages:

- *Left-handed (LH)* (e.g., [3, 12, 19, 20, 34, 40])—This is the terminology originally suggested by Veselago in [3]. It has the advantage of being related to the most fundamental property of these structures, which is antiparallel phase and group velocities (Section 2.1), and to be universal (applicable to 1D, 2D, and 3D structures). Some authors feel that the term "left-handed" could be confused with left-handed chiral materials, which may be considered a weakness of this term.
- *Double-negative (DNG)* (e.g., [28, 53])—In this case, the aforementioned potential confusion is not possible. However, this term does not tell what is negative and may be therefore seen as not self-consistent.
- *Negative-refractive-index (NRI)* (e.g., [38, 41])—NRI certainly represents a meaningful term for 2D or 3D structures and also has the advantage of emphasizing the effectively homogeneous nature of LH MTMs. However, it looses its sense in 1D LH structures, where propagation angles are not involved.
- *Backward-wave (BW)* (e.g., [32, 54])—The asset of this term may be that it points out the existence of antiparallel phase/group velocities, well known in conventional structures but fails to inform on the material (effectively homogeneous) nature of LH MTMs (Section 1.5).
- *Veselago medium* (e.g., [50, 51])—This choice pays tribute to the visionary idea of Veselago but does not provide any information on the properties of the medium.
- *Negative phase velocity medium (NPV)* (e.g., [52])—In our opinion, this term may be the best of all from a semantic point of view, but it has been so little used that it may be premature to adopt it definitely, unless some sort of consensus can be made between the main protagonists of MTM research.

In this book, we have made the choice of the terminology *left-handed (LH)* MTM.

1.7 TRANSMISSION LINE (TL) APPROACH

Although very exciting from a physics point of view, the initial TW-SRR MTMs (Fig 1.4) seem of little practical interest for engineering applications because

these structures are *resonant*, and consequently exhibit *high loss* and *narrow bandwidth*.[17] A structure made of resonating elements generally does not constitute a good transmission medium for a modulated signal because of the quality factor intrinsically associated with each resonator [57]. In a resonator, the loaded quality factor Q_l is related to the unloaded quality factor Q_u and external quality factor Q_e by the relation

$$\frac{1}{Q_l} = \frac{1}{Q_u} + \frac{1}{Q_e}, \tag{1.8}$$

which expresses the fact that the total transmission[18] loss ($\propto 1/Q_l$) through a resonator is equal to the sum of the dielectric/ohmic losses in the resonator ($\propto 1/Q_u$) and the coupling losses in the transitions with the external (source/load) circuits ($\propto 1/Q_e$). The loaded quality factor, which is the quantity actually measured and eventually relevant in terms of transmission, is also obtained from the magnitude of the transmission parameter (S_{21}) as

$$Q_l = \frac{f_r}{B}, \tag{1.9}$$

where f_r is the resonance frequency and B is the -3-dB bandwidth (in Hz), while the unloaded quality factor is defined as

$$Q_u = \omega \frac{\text{average energy stored in resonator}}{\text{power dissipated in resonator}}. \tag{1.10}$$

These textbook formulas show that, for given dielectric (dielectric loss $\propto \tan\delta$) and metal (ohmic loss $\propto 1/\sigma$, σ: conductivity) materials, there is an unavoidable *trade-off between bandwidth and transmission level*. Minimum transmission loss, or equivalently maximum Q_l, is achieved at the resonance frequency f_r by minimizing the bandwidth B, according to Eq. (1.9), because in this case very little power is dissipated in the cavity since its bandwidth is extremely narrow so that Q_u is maximized, according to Eq. (1.10)[19]. So, in this case, good transmission characteristics can be obtained. But bandwidth is so restricted that a modulated signal, even with a modest bandwidth, cannot be transmitted without distortion

[17]The insertion loss reported in [13] for the first TW-SRR structure was higher than 30 dB! Optimization of coupling mechanisms later improved the transmission characteristics of this structure. For instance, minimum transmission loss of around 1 dB over a 3-dB fractional bandwidth of 6.5% for a 3-cell structure was reported in [22]. Unfortunately, such performances are still not acceptable for microwave engineering applications.

[18]We are considering here a two-port TL-type (series) resonator system because we are interested in transmission characteristics through the structure. In such a system, a maximum in the magnitude of the transmission parameter (S_{21}) occurs at the resonance [57]. A perfectly loss-less resonating two-port system would correspond to $Q_l = \infty$, implying $Q_u = \infty$ and $Q_e = \infty$.

[19]This consideration is based on the assumption, generally reasonable, that $Q_e \gg Q_u$, so that Q_l is mostly dependent on Q_u, from (1.8).

through the resonating structure. Bandwidth can naturally be increased, but this immediately results in a decrease of Q_l according to Eq. (1.9) and therefore in an increase of transmission loss. In conclusion, a modulated signal cannot be transmitted efficiently through a resonating propagation medium. Although this statement is a very basic fact of resonators theory, it might not have been sufficiently appreciated in the physics community investigating MTMs.

Due to the weaknesses of resonant-type LH structures, there was a need for alternative architectures. Therefore, recognizing the analogy between LH waves and conventional backward waves (Section 1.5), three groups introduced, almost simultaneously in June 2002, a transmission line (TL) approach of metamaterials: Eleftheriades et. al [37, 55], Oliner [41] and Caloz et al. [39, 56].

In fact, hypothetical "backward-wave" uniform TLs, without any suggestion for a practical implementation!, had been briefly described in a few textbooks, such as [48]. The incremental circuit model for such a TL, which is essentially the *dual*[20] of a conventional right-handed (RH) series-L/shunt-C TL, is shown in Fig 1.7.[21,22]

The fundamental characteristics of the TL of Fig 1.7 are straightforwardly derived by elementary TL theory. Let us consider here for simplicity the lossless case, the lossy case being rigorously treated in Chapter 3. The complex

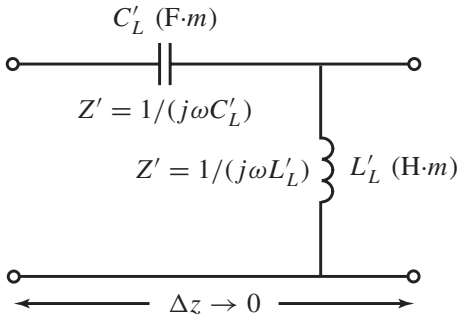

Fig. 1.7. Incremental circuit model for a hypothetical uniform LH TL.

[20]In this book, the term "dual" is considered in a broad sense, although more specific definitions are preferred by some electromagnetic theoreticians. The series-C/shunt-L prototype is called the dual of the series-L/shunt-C prototype, since it represents the fundamental "complement" to it, as corroborated by the fact is associated with negative refractive index as a complement of positive refractive index.

[21]In the present book, primes are used to represent reactances related to *per-unit-length* immittances, i.e., per-unit-length impedances Z' in Ω/m and admittances Y' in S/m.

[22]Note the units of L'_L (H·m) and C'_L (F·m) ensuring that Z' and Y' correspond to per-unit-length immittances in Ω/m and S/m, respectively. We have $Z(\Omega) = 1/[j\omega C_L(\text{F})] \to Z'(\Omega/\text{m}) = 1/[j\omega C_L(\text{F})\Delta z] = 1/[j\omega C'_L(\text{F·m})]$ where $C'_L = C_L \cdot \Delta z$; similarly, $Y(\text{S}) = 1/[j\omega L_L(\text{H})] \to Y'(\text{S/m}) = 1/[j\omega L_L(\text{H})\Delta z] = 1/[j\omega L'_L(\text{H}\cdot\text{m})]$ where $L'_L = L_L \cdot \Delta z$.

propagation constant γ, the propagation constant β, the characteristic impedance Z_c, the phase velocity v_p, and the group velocity v_g of the TL are given by

$$\gamma = j\beta = \sqrt{Z'Y'} = \frac{1}{j\omega\sqrt{L'_L C'_L}} = -j\frac{1}{\omega\sqrt{L'_L C'_L}}, \tag{1.11a}$$

$$\beta = -\frac{1}{\omega\sqrt{L'_L C'_L}} < 0, \tag{1.11b}$$

$$Z_c = \sqrt{\frac{Z'}{Y'}} = +\sqrt{\frac{L'_L}{C'_L}} > 0, \tag{1.11c}$$

$$v_p = \frac{\omega}{\beta} = -\omega^2\sqrt{L'_L C'_L} < 0, \tag{1.11d}$$

$$v_g = \left(\frac{\partial\beta}{\partial\omega}\right)^{-1} = +\omega^2\sqrt{L'_L C'_L} > 0. \tag{1.11e}$$

The last two equations immediately and unambiguously show that phase and group velocities in such a TL would be antiparallel, $v_p - \| v_g$. The phase velocity v_g, associated with the direction of phase propagation or wave vector $\boldsymbol{\beta}$, is negative, whereas the group velocity v_g, associated with the direction of power flow or Poynting vector $\mathbf{S}$, is positive (Section 2.1). Thus, the TL of Fig 1.7 is LH, according to the definition given in Section 1.2.

These considerations revealed that a LH TL medium could be engineered in a structural manner by conceiving LC structures corresponding to the model of Fig 1.6 *in condition that the average cell size p would be much smaller than the guided wavelength* λ_g ($p \ll \lambda_g$). If this could be accomplished, a *nonresonant* type, in the frequency range of interest, LH medium would be obtained. Such a design was shown to be perfectly realizable. The first practical LH TL was the microstrip structure shown in Fig 1.8(a) [39], with a 2D version of it in Fig 1.8(a).

Because of their nonresonant nature, TL MTMs can be designed to exhibit simultaneously *low loss* and *broad bandwidth*. Low loss is achieved by a "balanced" design (Section 1.8) of the structure and good matching to the excitation ports, whereas broad-bandwidth is a direct consequence of the TL nature of the structure and can be controlled by its LC parameters, which determine the cutoff frequency of the resulting high-pass structure. Another advantage of TL MTM structures is that they can be engineered in *planar configurations*, compatible with modern microwave integrated circuits (MICs). Finally, TL MTM structures can benefit from the efficient and well-established *TL theory* for the efficient design of microwave applications. Over 25 novel devices, with unique features or superior performances compared with conventional devices, have already been demonstrated [58, 59] and are described in the Chapters 3, 5 and 7.

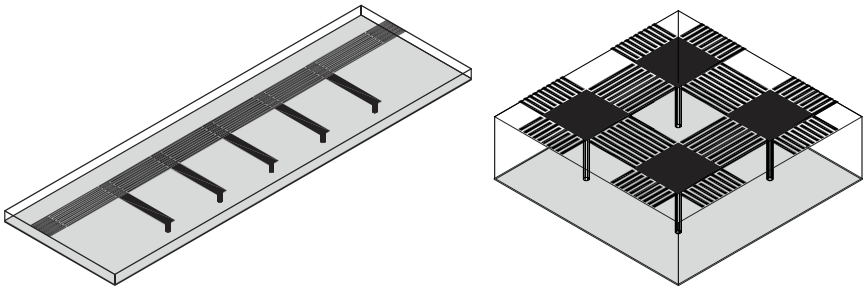

(a) (b)

Fig. 1.8. Planar transmission line (TL) LH structures in microstrip technology constituted of series interdigital capacitors and shunt stub inductors. The gray areas represent the ground planes, and the black surfaces represent metal. (a) 1D (e.g., [39, 40]). (b) 2D (similar to [44]).

1.8 COMPOSITE RIGHT/LEFT-HANDED (CRLH) MTMs

The concept of composite right/left-handed (CRLH) MTM, introduced by Caloz et al. in [58], is the cornerstone of the theory and applications presented in this book and is therefore extensively developed in the next chapters. However, this section already introduces this concept as a broad-band generalization of LH MTMs and provides a quick explanation of its essence.

The TL structures shown in Fig 1.8 are constituted of series (interdigital) capacitors C_L and shunt (stub) inductors L_L, intended to provide left-handedness from the explanations of the previous section. However, as a wave propagates along the structures, the associated currents and voltages induce other natural effects. As currents flow along C_L, magnetic fluxes are induced and therefore a series inductance L_R is also present; in addition, voltage gradients exist between the upper conductors and the ground plane, which corresponds to a shunt capacitance C_R. As a consequence, *a purely LH (PLH) structure does not exist*, even in a restricted frequency range, since a real LH structure necessarily includes (L_R, C_R) contributions in addition to the (L_L, C_L) reactances. This was the motivation for the introduction of the term "composite right/left-handed" (CRLH), allowing to account for the exact natural of practical LH media [58, 60].

The essential characteristics of a CRLH TL MTM can be inferred from analysis of the equivalent circuit of Fig 1.9(a). At low frequencies, L_R and C_R tend to be short and open, respectively, so that the equivalent circuit is essentially reduced to the series-C_L/shunt-L_L circuit, which is LH since it has antiparallel phase and group velocities; this LH circuit is of *highpass* nature; therefore, below a certain cutoff, a LH stopband is present. At high frequencies, C_L and L_L tend to be short and open, respectively, so that the equivalent circuit is essentially reduced to the series-L_R/shunt-C_R circuit, which is RH since it has parallel phase and group velocities; this LH circuit is of *lowpass* nature; therefore, above a certain cutoff, a RH stopband is present. In general, the series resonance ω_{se} and shunt

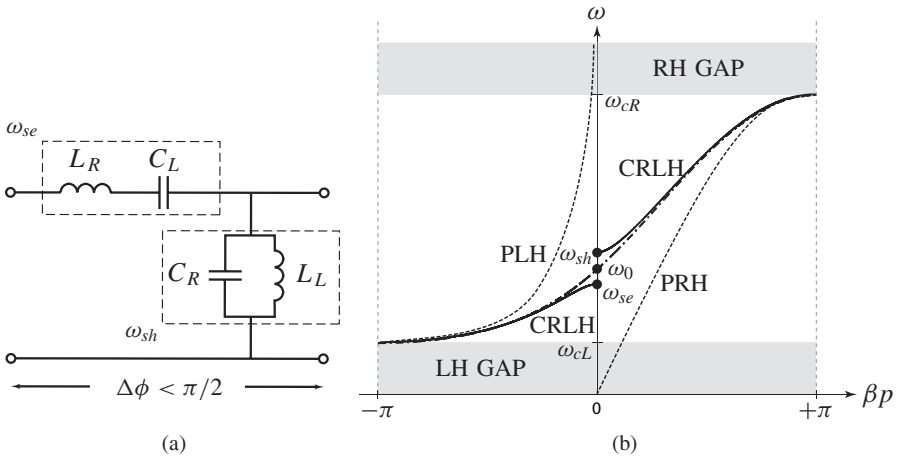

Fig. 1.9. Fundamentals of composite right/left-handed (CRLH) MTMs. (a) Unit cell TL prototype. (b) Dispersion diagram. The curves for a purely LH (PLH) structure ($L_R = C_R = 0$) and for a purely RH (PRH) structure ($L_L = C_L = \infty$) are also shown for comparison. Here, we have represented the case $\omega_{se} < \omega_{sh}$, but $\omega_{se} > \omega_{sh}$ is naturally also possible, depending on the LC parameters (Section 3.1).

resonance ω_{sh} are different, so that a gap exists between the LH and the RH ranges. However, if these resonances are made equal, or are "balanced," this gap disappears, and an *infinite-wavelength* ($\lambda_g = 2\pi/|\beta|$) propagation is achieved at the transition frequency ω_0. Despite its filter nature, the CRLH structure is never operated at the edges of the Brillouin zone, where $p \approx \lambda_g/2$, but only in the vicinity of the transition frequency, where effective-homogeneity is ensured ($p < \lambda_g/4$). Note that, although a CRLH structure has both a LH range and a RH range, the dispersion curve in each of these ranges significantly differs from that of the PLH and PRH structures, respectively, because of the combined effects of LH *and* RH contributions at all frequencies.

1.9 MTMs AND PHOTONIC BAND-GAP (PBG) STRUCTURES

The essential difference between MTM and photonic band gap (PBG) (or photonic crystals) structures has already been implicitly mentioned in Section 1.5 in connection with periodic structures. This section provides a more detailed explanation of this difference.

Photonic crystals [61] and PBG [62] structures are usually operated at frequencies where the lattice period p is of the order of a multiple of half a guided wavelength, $p \approx n\lambda_g/2$. In this case, as illustrated in Fig 1.10(a), the waves scattered by adjacent layers of the lattice interfere constructively for some specific angles of incidence. Therefore, net rejection of the incoming energy, corresponding to zero group velocity, occurs at these angles. This phenomenon is similar to

Bragg diffraction in X-ray optics [63] and is sometimes referred to as "Bragg-like" diffraction. The Bragg condition for maximum diffraction is given by

$$2p \sin\theta = m\lambda_g, \quad m = 0, 1, 2, \ldots, \tag{1.12}$$

where it is clearly seen that the Bragg angles are function of frequency (via λ_g). This condition, with $\beta = 2\pi/\lambda_g$, is equivalent to

$$\beta(\omega) = \frac{m\pi}{p \sin\theta(\omega)}, \quad m = 0, 1, 2, \ldots, \tag{1.13}$$

where the function $\beta(\omega)$ [or, more commonly, its inverse $\omega(\beta)$] is the *dispersion relation*, from which the *dispersion diagram* is computed. The points of the dispersion curves $\omega(\beta)$ where the Bragg condition is met have a zero slope (or tangent), since the slope of $\omega(\beta)$ corresponds to the group velocity, $v_g = d\omega/d\beta$, which is zero there. This means that Bragg points delimit the stop bands or *band gaps* in the dispersion diagram. The CRLH TL structure, whose dispersion diagram is shown in Fig 1.9(b), has two Bragg points: one is the highpass LH gap cutoff ω_{cL} and the other one is the lowpass RH gap cutoff ω_{cR}. At each of these two points, we have $|\beta|p = \pi$; i.e., $p = \pi/|\beta|$, which corresponds to (1.13) with $m = 1$.[23] These points correspond to resonating and noneffectively homogeneous frequencies, and are therefore *not in the range of MTM operation* of the CRLH structure.[24]

Whereas in a PBG structure period is of the order of wavelength [Fig 1.10(a)], period (or average period) in a MTM is much smaller than wavelength ($p/\lambda_g \ll 1$), as shown in Fig 1.10(b). Therefore, interference effects cannot take place in a MTM because the phase difference between adjacent cells is negligible. Instead, the wave simply travels through the material in a straight line, only probing average or effective constitutive parameters. This is what happens in the vicinity of the axis $\beta = 0$ (Γ spectral point) in a CRLH TL structure [Fig 1.9(b)]. In the balanced case, we have perfectly homogeneous transmission ($p/\lambda_g = 0$). In the unbalanced case, we have the two resonances ω_{se} and ω_{sh}. However, these resonances are *not Bragg* resonances but zeroth-order resonances (Section 5.5), in the sense that they are *infinite wavelength* ($\beta = 0$, fundamental mode) resonances.

Thus, a photonic crystal or PBG structure is operated in the Bragg regime, where periodicity plays a crucial role and the structure is strongly inhomogeneous, whereas a MTM is operated in the *long wavelength regime*, where the lattice does not need to be periodic and the structure is homogeneous. Consequently, (diffraction/scattering) *properties of photonic crystals are essentially determined by the lattice*,[25] *while the (refractive) properties of MTM are determined by the nature of the unit cell*, as detailed Section 3.1 [Eqs. (3.23) and (3.25)].

[23] In fact, $m = -1$ for the LH resonance, as it will be explained in Section 5.5.

[24] At these frequencies, the structure *is* a PBG but not a MTM.

[25] For instance, change the lattice of a 2D photonic crystal from square to hexagonal, without changing the unit cell or *basis*, results in dramatic changes in the PBG structure (dispersion diagram), whereas a change of the basis only hardly affects the PBG structure [61].

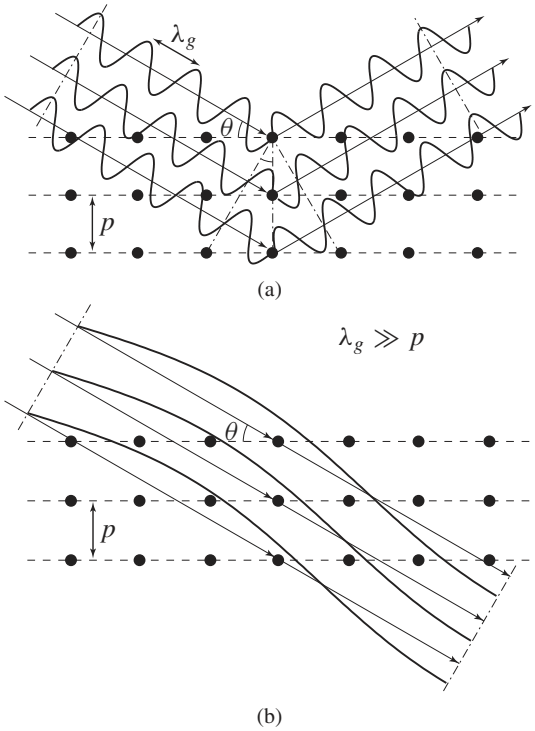

Fig. 1.10. Difference between the Bragg-scattering and long wavelength regimes. (a) Bragg regime, $p \approx \lambda_g/2$, usually prevailing in photonic crystals or PBG structures. (b) Long wavelength regime, $p \ll \lambda_g$, prevailing in MTMs.

Despite the fundamental differences pointed out above, several reports mentioning "negative refraction" in photonic crystals have been presented [64, 65, 66, 67].[26] The important distinction to make between these "refraction-like"crystals and LH MTMs is the following. A photonic crystal exhibits many higher-order modes (or bands) $\omega_m(\overline{\beta})$[27] with negative gradients $\nabla_{\overline{\beta}_m}\omega$ (m: mode index). For this reason, the corresponding m^{th} Fourier spectral contribution to the total field [Subsection 3.2.6, Eq. (3.107)] "propagates" with a phase in the opposite direction than that of power, which can result in NRI-like fields *outside* the photonic crystal (e.g., in a photonic crystal prism [67]). However, this "wave" $\overline{\beta}_m$ is only one Fourier component in the total physical field and is not this field itself. The physical field experiences scattering, not refraction, within the medium, as clearly shown in various reported simulations. No negative focusing would be possible

[26]It may be noted that the more careful term "refraction-like behavior" is used in [65].

[27]Note that $\overline{\beta}$ is a vector (hence the overline) if the dimension is superior than one. In the general 3D case, we have $\overline{\beta} = \beta_x\hat{x} + \beta_y\hat{y} + \beta_z\hat{z}$, where $\hat{x}, \hat{y}, \hat{z}$ denote unit vectors along the direction x, y, z, respectively.

inside a photonic crystal. In terms of engineering applications, this approach to obtain LH-like effects does not seem judicious because 1) such effects are more difficult to obtain in Bragg structures than in effectively homogeneous structures; 2) Bragg regime does not allow refractive effects inside the structure; and 3) Bragg structures necessarily result in large-size components since the unit cell itself is already very large, $p \sim m\lambda_g/2$.

1.10 HISTORICAL "GERMS" OF MTMs

In the previous sections, we reported the most significant milestones in the emergence of the new field of MTMs and more particularly of LH or CRLH MTMs. However, MTMs are related to such fundamental aspects of electromagnetic science and engineering that they necessarily had a few more or less diffuse "germs" in previous history. For instance in [68], Tretyakov presented an interesting "historical perspective," which uncovers some of these germs.[28] We give now a historical perspective partly inspired by this paper.

The earliest known speculation on negative refraction was made by Mandelshtam back in 1944 [69]. In this paper, Mandelshtam noticed that, given two media (labeled 1 and 2), for a given incidence angle θ_1 of the wave at the interface, Snell's law [Eq. (1.6a)] admits, mathematically, two solutions: not only the conventional solution θ_2 but also the "unusual" solution $\pi - \theta_2$[29]. Regarding this second solution, Mandelshtam wrote:

> "Demanding [as before] that the energy in the second medium propagates *from* the boundary, we arrive to the conclusion that the phase must propagate *towards* the boundary and, consequently, the propagation direction of the refracted wave will make with the normal the angle $\pi - \theta_2$. This derivation appears to be unusual, but of course there is no wonder because the phase velocity still tells us nothing about the direction of the energy transfer."

Although we note that Mandelshtam made no reference to *negative refraction* and did note carry out an in-depth study of this phenomenon, it is manifest that his argument refers to the same phenomenon. This fact reduces in no ways the pioneering merit of Veselago, who first addressed in 1967 the problem of LH materials in a systematic manner; Veselago may be considered as the father of LH MTMs with his decisive contribution of establishing their fundamental properties and predicting their unusual effects [3] (Section 1.2).

The year after his initial speculation (1945), with reference to Lamb (1904) who "gave examples of *fictitious* one-dimensional media with negative group velocity," Mandelshtam presented physical examples of structures supporting waves with "negative group velocity," such as structures with periodically varying

[28]The perspective of [68], as mentioned in the paper, is not systematic and therefore not necessarily exhaustive. It is likely that even former "germs" of MTMs have existed under various forms.

[29]This solution first seems to correspond to a ray in the half-plane of the reflection, but this solution is necessarily in medium 2, as Mandelshtam explained in the statement given here.

effective permittivity [70]. However, these structures were not MTMs in the sense defined in Section 1.1 but merely periodic structures, similar to those presented for example in [45, 46] at the same period, based on space harmonics excitation.

Maybe the first report of a hypothetical medium with simultaneously negative permittivity and permeability is the paper by Sivukhin in 1957 [71]. In this paper, Sivukhin noticed that a media with double negative parameters would be backward media, but this observation was still far from LH MTMs, as he pointed out "media with $\varepsilon < 0$ and $\mu < 0$ are not known. The question on the possibility of their existence has not been clarified."

As far as the TL approach of MTMs is concerned (Section 1.7), it has already been mentioned in Section 1.5 that LH TL circuit models with series capacitance and shunt inductances were used by several authors, such as for instance Brillouin and Pierce [45, 46], back in the 1940s in the context of periodic structures and microwave tubes. Malyuzhinets, in 1951, even showed a TL model similar to the CRLH TL model (Section 1.8) [47]. However, none of these approaches pertained to MTMs, as they were systematically used to describe space harmonics of periodic structures, as opposed to a fundamental propagation mode, and its seems that there was no clue at that time regarding how to design effective LH and CRLH TL structures. Moreover, most of the MTMs and CRLH MTM concepts presented in this book were apparently unknown. It should be noted that some authors, such as for instance Ramo et al., showed the PLH TL in their textbooks as a hypothetical effectively homogeneous TL, but without any suggestion on the existence or design of such TLs [48].

There is no doubt that the periodic slow-wave, backward-wave structures studied and developed in the 1940s and 1950s included important germs of MTMs and LH MTMs [45, 46, 47, 72]. It is worth noting that Silin discussed in 1959 the phenomenon of "negative refraction" in connection with periodic slow-wave structures (although the definition of a refractive index in a periodic structure operated in the Bragg regime is questionable, as pointed out in Section 1.9) [73]. Nowadays, there is still considerable effort in conceiving MTMs based on Bragg-regime periodic structures.

From the above reference with Mandelshtam, we see that Veselago was not the first to postulate the existence of LH media in [3], but it is an established fact that he was the first to conduct a systematic study of these media and to predict their most fundamental properties.

After Veselago, there has been made really no attempt to design a LH MTM before Smith et al. [4, 10]. However, resonant-type single ε negative and single μ negative structures, which are the constitutive elements of the SRR/TW LH MTMs (Section 1.3), have been reported under various forms long before the systematic studies of Pendry in [5] ($\varepsilon < 0$) and [6] ($\mu < 0$), who first developed a unified approach of these structure as effective media or MTMs. It seems that a wire medium, similar to the TW medium, was first described in the 1950s as a material for microwave lenses [74, 75]. Variants of the SRR were presented in the textbook by Schelkunoff and Friis published in 1952 [76], although these SRRs were not considered there as the artificial particles of a magnetic medium

(as introduced by Pendry in [6]). Media with loops of various shapes (e.g., omega, helix, spiral) were abundantly reported in the 1980s and 1990s in the investigation of artificial *chiral and bi-isotropic materials* for microwave applications [77]. These chiral materials are effective media and are therefore MTMs according to our definition (Section 1.1); negative permeability was identified theoretically and experimentally and described in several papers about chiral media. It is worth noting that a chiral medium with double-ring structure implants very similar to the SRRs was presented [78]. To conclude these remarks on relations between chiral and LH MTMs let us also note that backward waves have been recently shown to be supported by materials with positive parameters if chirality is present [79, 80].

REFERENCES

1. J.-S. G. Hong, M. J. Lancaster. *Microstrip Filters for RF/Microwave Applications,* Wiley-Interscience, 2001.
2. D. D. Stancil. *Theory of Magnetostatic Waves,* Springer-Verlag, 1993.
3. V. Veselago. "The electrodynamics of substances with simultaneously negative values of ε and μ," *Soviet Physics Uspekhi,* vol. 10, no. 4, pp. 509–514, Jan., Feb. 1968.
4. D. R. Smith, W. J. Padilla, D. C. Vier, S. C. Nemat-Nasser, and S. Schultz. "Composite medium with simultaneously negative permeability and permittivity," *Phys. Rev. Lett.,* vol. 84, no. 18, pp. 4184–4187, May 2000.
5. J. B. Pendry, A. J. Holden, W. J. Stewart, and I. Youngs. "Extremely low frequency plasmons in metallic mesostructure," *Phys. Rev. Lett.,* vol. 76, no. 25, pp. 4773–4776, June 1996.
6. J. B. Pendry, A. J. Holden, D. J. Robbins, and W. J. Stewart. "Low frequency plasmons in thin-wire structures," *J. Phys. Condens. Matter,* vol. 10, pp. 4785–4809, 1998.
7. J. B. Pendry, A. J. Holden, D. J. Robbins, and W. J. Stewart. "Magnetism from conductors and enhanced nonlinear phenomena," *IEEE Trans. Micr. Theory. Tech.,* vol. 47, no. 11, pp. 2075–1084, Nov. 1999.
8. M. Makimoto and S. Yamashita. *Microwave Resonators and Filters Communications: Theory, Design and Applications,* Springer, 2000.
9. D. R. Smith, D. C. Vier, N. Kroll, and S. Schultz. "Direct calculation of permeability and permittivity for a left-handed metamaterial," *App. Phys. Lett.,* vol. 77, no. 14, pp. 2246–2248, Oct. 2000.
10. R. A. Shelby, D. R. Smith, and S. Schultz. "Experimental verification of a negative index of refraction," *Science,* vol. 292, pp. 77–79, April 2001.
11. D. R. Smith and D. Schurig. "Electromagnetic wave propagation in media with indefinite permittivity and permeability tensors," *Phys. Rev. Lett.,* vol. 90, pp. 077405:1–4, Feb. 2003.
12. D. R. Smith, D. C. Vier, N. Kroll, and S. Schultz. "Direct calculation of permeability and permittivity for a left-handed metamaterial," *App. Phys. Lett.,* vol. 77, no. 14, pp. 2246–2248, Oct. 2000.

13. D. R. Smith and N. Kroll. "Negative refractive index in left-handed materials," *Phys. Rev. Lett.,* vol. 85, no. 14, pp. 2933–2936, Oct. 2000.
14. R. A. Shelby, D. R. Smith, S. C. Nemat-Nasser, and S. Schultz. "Microwave transmission through a two-dimensional, isotropic, left-handed metamaterial," *App. Phys. Lett.,* vol. 78, no. 4, pp. 489–491, Jan. 2001.
15. M. Garcia, and M. Nieto-Vesperinas. "Left-handed materials do not make a perfect lens," *Phys. Rev. Lett.,* vol. 88, no. 20, pp. 207403:1–4, Jan. 2002.
16. M. Garcia, and M. Nieto-Vesperinas. "Is there an experimental verification of a negative index of refraction yet?," *Optics Lett.,* vol. 27, no. 11, pp. 885–887, June 2002.
17. P. M. Valanju, R. M. Walser, and A. P. Valanju. "Wave refraction in negative-index media: always positive and very inhomogeneous," *Phys. Rev. Lett.,* vol. 88, no. 18, pp. 187401:1–4, 2002.
18. P. Gay-Balmaz and O. J. F. Martin. "Electromagnetic resonances in individual and coupled split-ring resonators," *J. App. Phys.,* vol. 92, no. 5, pp. 2929–2936, Sept. 2002.
19. R. Marqués, F. Median, and R. Rafii-El-Idrissi. "Role of bianisotropy in negative permeability and left-handed metamaterials," *Phys. Rev. B,* vol. 65, pp. 144440:1–6, 2002.
20. P. Markŏs and C. M. Soukoulis. "Numerical studies of left-handed materials and arrays of split ring resonators," *Phys. Rev. E,* vol. 65, pp. 036622:1–8, 2002.
21. P. Markŏs and C. M. Soukoulis. "Transmission studies of left-handed materials," *Phys. Rev. B,* vol. 65, pp. 033401:1–4, 2002.
22. R. B. Greegor, C. G. Parazzoli, K. Li, B. E. C. Koltenbah, and M. Tanielian. "Experimental determination and numerical simulation of the properties of negative index of refraction materials," *Optics Express,* vol. 11, no. 7, pp. 688–695, April 2003.
23. E. Ozbay, K. Aydin, E. Cubukcu, and M. Bayindir. "Transmission and reflection properties of composite double negative metamaterials in free space," *IEEE Trans. Antennas Propagat.,* vol. 51, no. 10, pp. 2592–2595, Oct. 2003.
24. C. R. Simovski, P. A. Belov, and S. He. "Backward wave region and negative material parameters of a structure formed by lattices of wires and split-ring resonators," *IEEE Trans. Antennas Propagat.,* vol. 51, no. 10, pp. 2582–2591, Oct. 2003.
25. R. Marqués, F. Mesa, J. Martel, and F. Median. "Comparative analysis of edge- and broadside-coupled split ring resonators for metamaterial: design, theory and experiments," *IEEE Trans. Antennas Propagat.,* vol. 51, no. 10, pp. 2572–2581, Oct. 2003.
26. R. W. Ziolkowski. "Design, fabrication, and testing of double negative metamaterials," *IEEE Trans. Antennas Propagat.,* vol. 51, no. 7, pp. 1516–1529, July 2003.
27. R. W. Ziolkowski and E. Heyman. "Wave propagation in media having negative permittivity and permeability" *Phys. Rev. E,* vol. 64, pp. 056625:1–15, 2001.
28. R. W. Ziolkowski. "Pulsed and CW gaussian beam interactions with double negative metamaterial slabs," *Optics Express,* vol. 11, no. 7, pp. 662–681, April 2003.
29. C. Caloz, C. C. Chang, and T. Itoh. "Full-wave verification of the fundamental properties of left-handed materials (LHMs) in waveguide configurations" *J. App. Phys.,* vol. 90, no. 11, pp. 5483–5486, Dec. 2001.
30. P. P. M. So and W. J. R. Hoefer. "Time domain TLM modeling of metamaterials with negative refractive index," *IEEE-MTT Int'l Symp.,* pp. 1779–1782, Fort Worth, TX, June 2004.

31. P. P. M. So, H. Du, and W. J. R. Hoefer. "Modeling of metamaterials with negative refractive index using 2D-shunt and 3D-SCN TLM networks," *IEEE Trans. Microwave Theory Tech.,* pp. 1496–1505 vol. 53, no. 4, April. 2005.

32. I. V. Lindell, S. A. Tretyakov, K. I. Nikoskinen, and S. Ilvonen. "BW media –media with negative parameters, capable of supporting backward waves," *Micr. Opt. Technol. Lett.,* vol. 31, no. 2, pp. 129–133, Oct. 2001.

33. J. A. Kong, B.-I. Wu, and Y. Zhang. "A unique lateral displacement of a Gaussian beam transmitted through a slab with negative permittivity and permeability," *Micr. Opt. Technol. Lett.,* vol. 33, no. 2, pp. 136–139, April 2002.

34. J. Pacheco, T. M. Grzegorzcyk, B.-I. Wu, Y. Zhang, and J. A. Kong. "Wave propagation in homogeneous isotropic frequency-dispersive left-handed media," *Phys. Rev. Lett.,* vol. 89, no. 25, pp. 257401:1–4, Dec. 2002.

35. D. R. Smith, D. Schurig, and J. B. Pendry. "Negative refraction of modulated electromagnetic waves," *App. Phys. Lett.,* vol. 81, no. 15, pp. 2713–2715, Oct. 2002.

36. M. W. McCall, A. Lakhtakia, and W. S. Weiglhofer. "The negative index of refraction demystified," *Eur. J. Phys.,* vol. 23, pp. 353–359, 2002.

37. A. K. Iyer and G. V. Eleftheriades. "Negative refractive index metamaterials supporting 2-D waves," in *IEEE-MTT Int'l Symp.,* vol. 2, Seattle, WA, pp. 412–415, June 2002.

38. G. V. Eleftheriades, A. K. Iyer, and P. C. Kremer. "Planar negative refractive index media using periodically L-C loaded transmission lines," *IEEE Trans. Microwave Theory Tech.,* vol. 50, no. 12, pp. 2702–2712, Dec. 2002.

39. C. Caloz and T. Itoh. "Application of the transmission line theory of left-handed (LH) materials to the realization of a microstrip LH transmission line," *in Proc. IEEE-AP-S USNC/URSI National Radio Science Meeting,* vol. 2, San Antonio, TX, pp. 412–415, June 2002.

40. C. Caloz and T. Itoh. "Transmission line approach of left-handed (LH) structures and microstrip realization of a low-loss broadband LH filter," *IEEE Trans. Antennas Propagat.,* vol. 52, no. 5, pp. 1159–1166, May 2004.

41. A. A. Oliner. "A periodic-structure negative-refractive-index medium without resonant elements," in *URSI Digest, IEEE-AP-S USNC/URSI National Radio Science Meeting,* San Antonio, TX, pp. 41, June 2002.

42. A. A. Oliner. "A planar negative-refractive-index medium without resonant elements," in *IEEE-MTT Int'l Symp.,* Philadelphia, PA, pp. 191–194, June 2003.

43. A. K. Iyer, P. C. Kremer, and G. V. Eleftheriades. "Experimental and theoretical verification of focusing in a large, periodically loaded transmission line negative refractive index metamaterial," *Optics Express,* vol. 11, no. 7, pp. 696–708, April 2003.

44. A. Sanada, C. Caloz, and T. Itoh. "Planar distributed structures with negative refractive index," *IEEE Trans. Microwave Theory Tech.,* vol. 52, no. 4, pp. 1252–1263, April 2004.

45. L. Brillouin. *Wave Propagation in Periodic Structures,* McGraw-Hill, 1946.

46. J. R. Pierce. *Traveling-Wave Tubes,* D. Van Nostrand, 1950.

47. G. D. Malyuzhinets. "A note on the radiation principle," *Zhurnal Technicheskoi Fiziki,* vol. 21, pp. 940–942, 1951 [in Russian].

48. S. Ramo, J. R. Whinnery and T. Van Duzer. *Fields and Waves in Communication Electronics,* Third Edition, John Wiley & Sons, 1994.

49. J. A. Kong. *Electromagnetic Wave Theory,* Second Edition, EMW Pub., 2000.
50. P. A. Belov. "Backward waves and negative refraction in uniaxial dielectrics with negative dielectric permittivity along the anisotropy axis," *Microwave Opt. Technol. Lett.,* vol. 37, no. 4, pp. 259–263, March 2003.
51. D. Felbacq and A. Moreau. "Direct evidence of negative refraction media with negative ε and μ," *J. Opt. A,* vol. 5, pp. L9–L11, 2003.
52. A. Lakhtakia. "Positive and negative Goos-H anchen shifts and negative phase-velocity mediums (alias left-handed materials)," *Int. J. Electron. Commun.,* vol. 58, no. 3, pp. 229–231, 2004.
53. A. Alù and N. Engheta. "Guided modes in a waveguide filled with a pair of single-negative (SNG), double-negative (DNG) and/or double-positive (DPS) layers," *IEEE Trans. Microwave Theory Tech.,* vol. 52, no. 1, pp. 192–210, Jan. 2004.
54. S. A. Tretyakov, S. I. Maslovski, I. S. Nefedov, M. K. Kärkkäinen. "Evanescent modes stored in cavity resonators with backward-wave slabs," *Microwave Opt. Technol. Lett.,* vol. 38, no. 2, pp. 153–157, May 2003.
55. A. Grbic and G. V. Eleftheriades. "A backward-wave antenna based on negative refractive index L-C networks," in *Proc. IEEE-AP-S USNC/URSI National Radio Science Meeting,* vol. 4, San Antonio, TX, pp. 340–343, June 2002.
56. C. Caloz, H. Okabe, T. Iwai, and T. Itoh. "Anisotropic PBG surface and its transmission line model," in *URSI Digest, IEEE-AP-S USNC/URSI National Radio Science Meeting,* San Antonio, TX, pp. 224, June 2002.
57. R. E. Collin. *Foundations for Microwave Engineering,* Second Edition, McGraw-Hill, 1992.
58. C. Caloz and T. Itoh. "Novel microwave devices and structures based on the transmission line approach of meta-materials," in *IEEE-MTT Int'l Symp.,* vol. 1, Philadelphia, PA, pp. 195–198, June 2003.
59. A. Lai, C. Caloz and T. Itoh. "Transmission line based metamaterials and their microwave applications," *Microwave Mag.,* vol. 5, no. 3, pp. 34–50, Sept. 2004.
60. A. Sanada, C. Caloz and T. Itoh. "Characteristics of the composite right/left-handed transmission lines," *IEEE Microwave Wireless Compon. Lett.,* vol. 14, no. 2, pp. 68–70, Feb. 2004.
61. J. D. Joannopoulos, R. D. Meade, J. N. Winn. *Photonic Crystals,* Princeton University Press, 1995.
62. "Special issue on photonic band-gap structures," *Trans. Microwave Theory Tech.,* vol. 47, no. 11, Nov. 1999.
63. C. Kittel. *Introduction to Solid State Physics,* Seventh Edition, Wiley, 1995.
64. B. Gralak, S. Enoch, and G. Tayeb. "Anomalous refractive properties of photonic crystals," *J. Opt. Soc. Am.,* vol. 17, no. 6, pp. 1012–1020, June 2000.
65. M. Notomi. "Theory of light propagation in strongly modulated photonic crystals: refraction-like behavior in the vicinity of the photonic band gap," *Phys. Rev. B,* vol. 62, no. 16, pp. 10696–10705, Oct. 2000.
66. C. Luo, S. G. Johnson, J. D. Joannopoulos, and J. B. Pendry. "All-angle negative refraction without negative effective index," *Phys. Rev. B,* vol. 65, pp. 201104:1–4, 2002.
67. P. V. Parimi, W. T. Lu, P. Vodo, J. Sokoloff, J. S. Devov, and S. Sridhar. "Negative refraction and left-handed electromagnetism in microwave photonic crystals," *Phys. Rev. Lett.,* vol. 92, no. 12, pp. 127401:1–4, June 2004.

68. S. A. Tretyakov. "Research on negative refraction and backward-wave media: a historical perspective," in *Proc. Latsis Symposium,* Lausanne, Switzerland, pp. 30–35, March 2005.

69. L. I. Mandelshtam. "Lecture on some problems of the theory of oscillations," in *Complete Collection of Works,* vol. 5, Moscow: Academy of Sciences, pp. 428–467, 1944 [in Russian].

70. L. I. Mandelshtam. "Group velocity in a crystal lattice," in *Zhurnal Eksperimentalnoi i Teoreticheskoi Fiziki,* vol. 15, n. 9, pp. 476–478, 1945 [in Russian].

71. D. V. Sivukhin. "The energy of electromagnetic waves in dispersive media," in *Opt. Spektrosk.,* vol. 3, pp. 308–312, 1957.

72. R. G. E. Hutter. *Beam and Wave Electronics in Microwave Tubes,* Van Nostrand, 1960.

73. R. A. Silin. "Waveguiding properties of two-dimensional periodical slow-wave systems," in *Voprosy Radioelectroniki, Electronika,* vol. 4, pp. 11–33, 1959.

74. J. Brown. "Artificial dielectrics," in *Progress in Dielectrics,* vol. 2, pp. 195–225, 1960.

75. W. Rotman. "Plasma simulation by artificial and parallel plate media," in *IRE Trans. Ant. Propagat.,* vol. 10, pp. 82–95, 1962.

76. S. A. Schelkunoff and H. T. Friis. *Antennas: Theory and Practice,* John Wiley & Sons, 1952.

77. A. H. Sihvola, A. J. Viitanen, I. V. Lindell, and S. A. Tretyakov. *Electromagnetic Waves in Chiral and Bi-Isotropic Media,* Artech House, 1994.

78. M. V. Kostin and V. V. Shevchenko. "Artificial magnetics based on double circular elements," in Proc. *Bioanisotropics '94,* Périgueux, France, pp. 46–56, 1994.

79. S. Tretyakov, I. Nefedov, A. Sihvola, S. Maslovski, and C. Simovski. "Waves and energy in chiral nihility," *Journal of Electromagnetic Waves and Applications,* vol. 17, no. 7, pp. 695–706, 2003.

80. J. Pendry. "A chiral route to negative refraction," *Science,* vol. 306, pp. 1353–1955, 2004.

2

FUNDAMENTALS OF LH MTMs

Chapter 2 presents a concise overview on the fundamental theory of left-handed (LH) metamaterials (MTMs). Whereas this theory is of paramount importance in the study of any MTM or MTM-based structure, most of the MTM properties discussed here have not been directly exploited in practical applications yet.[1] However, it is useful still to describe them, for the sake of both completeness and illustration of the richness and wealth of potential applications, probably extending far beyond those presented in this book.

Section 2.1 shows how the antiparallelism existing between the phase and group velocities in a LH medium is inferred from Maxwell's equations and leads to negative refractive index (NRI). Section 2.2 demonstrates that a LH medium is necessarily frequency-dispersive and establishes the subsequent necessary entropy conditions on the LH constitutive parameters. Section 2.3 describes the modified boundary conditions at the interface between a right-handed (RH) medium and a LH medium compared with those at the boundary between two RH media. The next sections describe the reversals of the Doppler effect (Section 2.4) and the Vavilov-Čerenkov radiation (Section 2.5) occurring in LH media. The most important phenomenon, which is the reversal of Snell's law associated with NRI,

[1]We are referring essentially to refractive properties of 2D (or possibly 3D) MTM (Section 7.3), which are still mostly restricted to concepts at the time of this writing. This is in contrast to the properties exploited in the majority of the applications presented in this book, which are generally based on the CRLH TL concept (Section 1.8), not necessarily requiring refractive properties (at least not in 1D structures, where angles are not involved).

Electromagnetic Metamaterials: Transmission Line Theory and Microwave Applications,
By Christophe Caloz and Tatsuo Itoh

is presented in Section 2.6, which is followed by a section describing the LH "flat lens" (Section 2.7). Fresnel coefficients are given and discussed in Section 2.8. The next two sections describe the reversal of the Goos-Hänchen effect (Section 2.9) at a RH-LH interface and the reversal of the convergence/divergence effects induced by (curved) LH convex/concave lenses (Section 2.10). Finally, the concept of subwavelength diffraction is described in Section 2.11.

2.1 LEFT-HANDEDNESS FROM MAXWELL'S EQUATIONS

A LH material is an electromagnetic medium with *simultaneously negative permittivity ε and permeability μ*. We will show that the double negative nature of the constitutive parameters, ε and μ, results in the propagation of electromagnetic waves exhibiting *antiparallel phase and group velocities*[2] or LH waves. For this purpose, we start by writing Maxwell's equations[3]

$$\nabla \times \overline{\mathcal{E}} = -\frac{\partial \overline{\mathcal{B}}}{\partial t} - \overline{\mathcal{M}_s}, \quad \text{(Faraday's law)} \tag{2.1a}$$

$$\nabla \times \overline{\mathcal{H}} = \frac{\partial \overline{\mathcal{D}}}{\partial t} + \overline{\mathcal{J}_s}, \quad \text{(Ampere's law)} \tag{2.1b}$$

$$\nabla \cdot \overline{\mathcal{D}} = \varrho_e, \quad \text{(electric Gauss' law)} \tag{2.1c}$$

$$\nabla \cdot \overline{\mathcal{B}} = \varrho_m, \quad \text{(magnetic Gauss' law)} \tag{2.1d}$$

where $\overline{\mathcal{E}}$ (V/m) is the electric field intensity, $\overline{\mathcal{H}}$ (A/m) is the magnetic field intensity, $\overline{\mathcal{D}}$ (C/m^2) is the electric flux density, $\overline{\mathcal{B}}$ (W/m^2) is the magnetic flux density, $\overline{\mathcal{M}_s}$ (V/m^2) is the (fictitious) magnetic current density, $\overline{\mathcal{J}_s}$ (A/m^2) is the electric current density, ϱ_e (C/m^3) is the electric charge density, and ϱ_m (C/m^3) is the (fictitious) magnetic charge density. In addition, if the medium is linear (ε, μ not depending on $\overline{E}$ or $\overline{H}$) and nondispersive[4] (ε, μ not depending on ω), the vectors in the pairs $[\overline{\mathcal{D}}, \overline{\mathcal{E}}]$ and $[\overline{\mathcal{B}}, \overline{\mathcal{H}}]$ are related by the constitutive equations

$$\overline{\mathcal{D}} = \varepsilon_0 \overline{\mathcal{E}} + \overline{\mathcal{P}} = \varepsilon_0(1 + \chi_e)\overline{\mathcal{E}} = \varepsilon_0 \varepsilon_r \overline{\mathcal{E}} = \varepsilon \overline{\mathcal{E}}, \tag{2.2a}$$

$$\overline{\mathcal{B}} = \mu_0 \overline{\mathcal{H}} + \overline{\mathcal{M}} = \mu_0(1 + \chi_m)\overline{\mathcal{H}} = \mu_0 \mu_r \overline{\mathcal{H}} = \mu \overline{\mathcal{H}}, \tag{2.2b}$$

[2]Antiparallel vectors are collinear vectors with opposite signs, i.e., opposite directions.

[3]For the sake of generality, we consider here generalized symmetrical Maxwell's equations, including fictitious magnetic current density and magnetic charge density. Fictitious magnetic conductivity will also be admitted in the constitutive relations.

[4]In fact, LH media are necessarily dispersive, as shown in Section 2.2, where the corresponding constitutive relations and subsequent entropy conditions will be derived. However, Eqs. (2.2) are approximately true in a weakly dispersive media. (In practice, many dispersive media can be considered weakly dispersive.) In this section, we will assume weakly nondispersive LH media before presenting a rigorous discussion including dispersion in Section 2.2.

where $\overline{\mathcal{P}} = \varepsilon_0 \chi_e$ and $\overline{\mathcal{M}} = \mu_0 \chi_m$ are the electric and magnetic polarizations, respectively, χ_e and χ_m are the electric and magnetic susceptibilities, respectively, $\varepsilon_0 = 8.854 \cdot 10^{-12}$ (F/m) and $\mu_0 = 4\pi \cdot 10^{-7}$ (H/m) are the permittivity and permeability of free space, respectively, and $\varepsilon_r = 1 + \chi_e$ and $\mu_r = 1 + \chi_m$ are the permittivity and permeability, respectively, of the material considered. The latter can be written in the form

$$\varepsilon_r = \varepsilon' - j\varepsilon'' = \varepsilon'(1 - j\tan\delta_e), \quad \tan\delta_e = \frac{\omega\varepsilon'' + \sigma_e}{\omega\varepsilon'}, \tag{2.3a}$$

$$\mu_r = \mu' - j\mu'' = \mu'(1 - j\tan\delta_m), \quad \tan\delta_m = \frac{\omega\mu'' + \sigma_m}{\omega\mu'}. \tag{2.3b}$$

In the last two equations, the imaginary parts of ε and μ account for losses: $\omega\varepsilon''$ represents loss due to dielectric damping, σ_e loss due to finite electric conductivity, $\omega\mu''$ loss due to magnetic damping, and σ_m loss due to finite (fictitious) magnetic conductivity. Assuming harmonic fields with the time dependence[5] $e^{+j\omega t}$ and defining the corresponding generic phasor $\overline{F}(\overline{r})$ as

$$\overline{\mathcal{F}}(\overline{r}, t) = \mathrm{Re}\left[\overline{F}(\overline{r})e^{+j\omega t}\right], \tag{2.4}$$

where $\overline{\mathcal{F}}$ represents any of the physical quantities in Eq. (2.1), Maxwell's equations and the constitutive equations can be written as

$$\nabla \times \overline{E} = -j\omega\mu\overline{H} - \overline{M}_s, \tag{2.5a}$$

$$\nabla \times \overline{H} = j\omega\varepsilon\overline{E} + \overline{J}_s, \tag{2.5b}$$

$$\nabla \cdot \overline{D} = \rho_e, \tag{2.5c}$$

$$\nabla \cdot \overline{B} = \rho_m, \tag{2.5d}$$

and

$$\overline{D} = \varepsilon\overline{E}, \tag{2.6a}$$

$$\overline{B} = \mu\overline{H}, \tag{2.6b}$$

respectively. Let us consider now the *plane wave*

$$\overline{E} = \overline{E}_0 e^{-j\overline{\beta}\cdot\overline{r}}, \tag{2.7a}$$

$$\overline{H} = \frac{\overline{E}_0}{\eta} e^{-j\overline{\beta}\cdot\overline{r}}, \tag{2.7b}$$

[5]The dependence $e^{+j\omega t}$ is the convention of engineers, whereas physicists generally use the phasor time dependence $e^{-i\omega t}$. Conversion from one formulation to the other can be accomplished by the imaginary variable substitution $i \to -j$. Particular care must be taken to this divergence of conventions in the study of LH media, where sign often plays a crucial role.

where $\eta = |\overline{E}|/|\overline{H}|$ denotes the wave impedance. Because any physical quantity can be expressed as a superposition of plane waves by virtue of the Fourier transform, consideration of an isolated plane wave will provide information on the fundamental response of the medium. This information is straightforwardly obtained by substituting the plane wave expressions (2.7) into the first two Maxwell's equations [Eq. (2.5)].

For simplicity, let us consider a loss-less medium[6] ($\varepsilon'' = \mu'' = 0$) in regions without sources ($\overline{M}_s = \overline{J}_s = 0$). In the case of a RH medium, $\varepsilon, \mu > 0$, and therefore

$$\overline{\beta} \times \overline{E} = +\omega\mu\overline{H}, \tag{2.8a}$$

$$\overline{\beta} \times \overline{H} = -\omega\varepsilon\overline{E}, \tag{2.8b}$$

which builds the familiar *right-handed* triad $(\overline{E}, \overline{H}, \overline{\beta})$ shown in Fig 2.1(a). In contrast, in the case of a LH medium, $\varepsilon, \mu < 0$, and therefore, since $|\varepsilon| = -\varepsilon > 0$ and $|\mu| = -\mu > 0$,

$$\overline{\beta} \times \overline{E} = -\omega|\mu|\overline{H}, \tag{2.9a}$$

$$\overline{\beta} \times \overline{H} = +\omega|\varepsilon|\overline{E}, \tag{2.9b}$$

which builds the unusual *left-handed* triad $(\overline{E}, \overline{H}, \overline{\beta})$ shown in Fig 2.1(b).

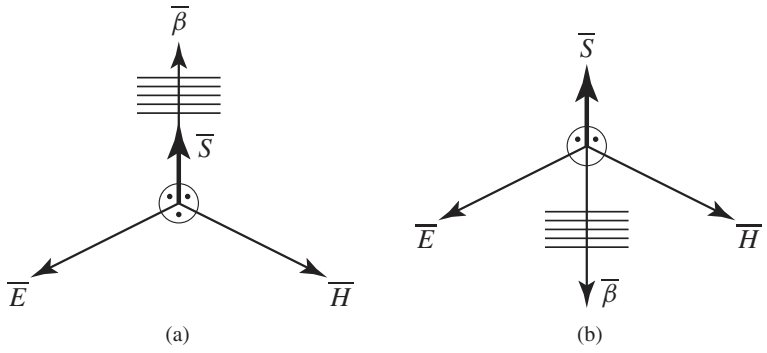

Fig. 2.1. Electric field–magnetic field–wave vector triad $(\overline{E}, \overline{H}, \overline{\beta})$ and Poynting vector $\overline{S}$ for an electromagnetic wave, as prescribed by Maxwell's equations [Eq. (2.1)] and Poynting's theorem [Eq. (2.19)], respectively. (a) Conventional, right-handed (RH) medium, where $\varepsilon, \mu > 0$. (b) Left-handed (LH) medium, where $\varepsilon, \mu < 0$.

[6]The following argument holds in the lossy case, because ε'' and μ'' represent an attenuation factor in Eq. (2.7), which is related to the evanescent nature of the wave and therefore does not affect phase in any way.

Thus, frequency being always a positive quantity, the phase velocity

$$\overline{v}_p = \frac{\omega}{\beta}\hat{\beta}, \quad \left(\hat{\beta} = \overline{\beta}/|\overline{\beta}|\right) \tag{2.10}$$

in a LH medium [Eq. (2.8)] is opposite to the phase velocity in a RH medium [Eq. (2.9)]. Moreover, because the wave number β is known to be positive in a RH medium (outward propagation from the source), it is negative in a LH medium (inward propagation to the source):

$$\text{RH medium: } \beta > 0 \quad (v_p > 0), \tag{2.11a}$$

$$\text{LH medium: } \beta < 0 \quad (v_p < 0). \tag{2.11b}$$

For generality, Eqs. (2.8) and (2.9) can be compacted into the single relation

$$\overline{\beta} \times \overline{E} = s\omega|\mu|\overline{H}, \tag{2.12a}$$

$$\overline{\beta} \times \overline{H} = -s\omega|\varepsilon|\overline{E}, \tag{2.12b}$$

where s is a "handedness" sign function defined as

$$s = \begin{cases} +1 & \text{if the medium is RH,} \\ -1 & \text{if the medium is LH.} \end{cases} \tag{2.13}$$

It follows from Eq. (2.9) [or Eq. (2.12) with $s = -1$] and Fig 2.1(b) that, in LH medium phase, which is related to phase velocity v_p, propagates backward to the source in the opposite direction than that of power, related to group velocity v_g. With the adopted time dependence $e^{+j\omega t}$ and assuming that power propagates in the direction of positive values of the space variable r, this backward-wave propagation implies that the fields have a time-space dependence

$$\overline{E}, \overline{H} \approx e^{+j(\omega t + |n|k_0 r)}. \tag{2.14}$$

In this expression, transverse electromagnetic (TEM) propagation, prevailing in a homogeneous and isotropic medium, has been implicitly assumed, so that the propagation constant has only one component that is equal to the wave number k_n in the medium

$$\beta = k_n = nk_0 = n\frac{\omega}{c}, \tag{2.15}$$

where

$$n = \pm\sqrt{\varepsilon_r \mu_r} \tag{2.16}$$

is the refractive index [Eq. (1.1)]. In a LH medium, since $\beta < 0$, we must have from Eqs. (2.15) and (2.16) a negative index of refraction (NRI), $n < 0$ (so that

$|n| = -n$). This demonstrates that *the index of refraction is negative in a medium with negative permittivity and permeability*. The index of refraction can thus be written in general as

$$n = s\sqrt{\varepsilon_r \mu_r}, \tag{2.17}$$

where Eq. (2.13) was used.

To better understand the implications of the above observations, let us consider also the Poynting theorem, which reads for the volume shown in Fig 2.2 [1]

$$P_s = P_0 + P_l + 2j\omega(W_e - W_m), \tag{2.18a}$$

where

$$P_s = -\frac{1}{2}\int_V \left(\overline{E}\cdot\overline{J}_s^* + \overline{H}^*\cdot\overline{M}_s\right) dv, \tag{2.18b}$$

$$P_0 = \frac{1}{2}\oint_S \overline{E}\times\overline{H}^*\cdot d\overline{s}, \tag{2.18c}$$

$$P_l = \frac{\sigma_e}{2}\int_V |\overline{E}|^2 dv + \frac{\sigma_m}{2}\int_V |\overline{H}|^2 dv + \frac{\omega}{2}\int_V \left(\varepsilon''|\overline{E}|^2 + \mu''|\overline{H}|^2\right) dv, \tag{2.18d}$$

$$W_e = \frac{1}{4}\mathrm{Re}\int_V \overline{E}\cdot\overline{D}^* dv, \tag{2.18e}$$

$$W_m = \frac{1}{4}\mathrm{Re}\int_V \overline{H}\cdot\overline{B}^* dv. \tag{2.18f}$$

This theorem expresses the complex power P_s in a volume V delivered by the sources $\overline{M}_s$ and $\overline{J}_s$ in terms of the complex power flow P_0 out of the closed surface S delimiting V, the time-average dissipated power P_l in V due to electric/magnetic conductivities, dielectric and magnetic losses, and the time average

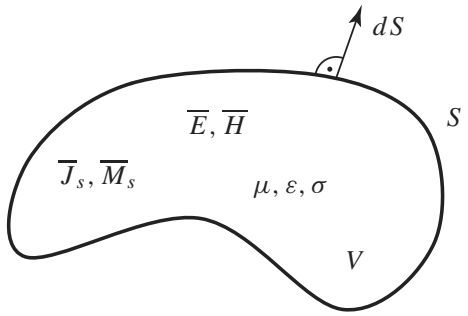

Fig. 2.2. Volume V formed by the closed surface S and containing the field intensities $\overline{E}, \overline{H}$ and the sources $\overline{J}_s$, $\overline{M}_s$.

electric and magnetic energy stored in V, W_e, and W_m, respectively. The power flow P_0 is related to the Poynting vector $\overline{S}$, defined as[7]

$$\overline{S} = \overline{E} \times \overline{H}^*, \tag{2.19}$$

The Poynting vector $\overline{S}$, associated with the power flow P_0 in Eq. (2.18c), is oriented toward the direction of propagation of energy over time and is therefore *parallel* to the group velocity

$$\overline{v}_g = \nabla_{\overline{\beta}} \omega, \tag{2.20}$$

which may be broadly defined as the velocity of a modulated signal in a distortionless medium. Thus, in contrast to the wave vector $\overline{\beta}$, the Poynting vector is *not* dependent on the constitutive parameters of the medium (ε and μ), but only on $\overline{E}$ and $\overline{H}$. This conclusion completes the characterization of the RH and LH media (Fig 2.1), which may be summarized as follows, considering positive the direction of the power flow

$$\text{RH medium:} \quad v_p > 0 \ (\beta > 0) \quad \text{and} \quad v_g > 0, \tag{2.21a}$$

$$\text{LH medium:} \quad v_p < 0 \ (\beta < 0) \quad \text{and} \quad v_g > 0. \tag{2.21b}$$

The fact that phase velocity is negative ($v_p < 0$) might seem troubling at first glance. However, this appears more acceptable if one remembers that phase velocity simply corresponds to the propagation of a *perturbation* and not of energy [2]. In contrast, a negative group velocity ($v_g < 0$) would violate causality, as it would correspond to transfer of energy toward the source! If often negative-gradient dispersion curves $\omega(\overline{\beta})$ associated with positive values of $\overline{\beta}$ (i.e., apparently negative group velocity modes) are observed in standard representations of dispersion diagrams, these curves should be interpreted as the eigen-solutions of the wave equation corresponding to the situation where the source placed at the other end of the medium (energy transfer from positive to negative values of the space variable).

2.2 ENTROPY CONDITIONS IN DISPERSIVE MEDIA

In this section, we will show that a LH medium, in contrast to a RH medium, is necessarily frequency dispersive, and we will derive a corresponding frequency-domain dispersion condition, called the entropy condition, which must be satisfied by the LH constitutive parameters ε and μ.

A *frequency-dispersive* or simply *dispersive* medium is a medium in which the propagation constant (β) is a nonlinear function of frequency, which results in

[7]This expression also holds in a LH (dispersive) medium, as shown in Section 2.2.

frequency-dependent group velocity and leads to distortion of modulated signals.[8] This implies from Eqs. (2.15) and (2.16) that either ϵ_r or μ_r (or both) have to be functions of frequency. An equivalent, more fundamental, definition is the following: dispersive medium is a medium in which the relation between $\overline{\mathcal{D}}/\overline{\mathcal{B}}$ and $\overline{\mathcal{E}}/\overline{\mathcal{H}}$[9] is a dynamic relation with "memory" rather than an instantaneous relation. The field intensities $\overline{\mathcal{E}}/\overline{\mathcal{H}}$ "create" the flux densities $\overline{\mathcal{D}}/\overline{\mathcal{B}}$ by inducing oscillation of the bound electrons in the atoms of the medium. These electrons respond to the excitation ($\overline{\mathcal{E}}/\overline{\mathcal{H}}$) with various delays to produce the collective response ($\overline{\mathcal{D}}/\overline{\mathcal{B}}$) of the system. As a consequence, a time delay exists between the cause and the effect, and arbitrary field intensities $\overline{\mathcal{E}}(t)/\overline{\mathcal{H}}(t)$ induce flux densities $\overline{\mathcal{D}}(t)/\overline{\mathcal{B}}(t)$ that are superpositions (assuming a linear medium) of the effects of $\overline{\mathcal{E}}(t')/\overline{\mathcal{H}}(t')$ at all times $t' \leq t$. This corresponds to the convolutions[10]

$$\overline{\mathcal{D}}(\overline{r}, t) = \varepsilon(t) * \overline{\mathcal{E}}(\overline{r}, t) = \int_{-\infty}^{t} \varepsilon(t - t')\overline{\mathcal{E}}(\overline{r}, t')dt', \tag{2.22a}$$

$$\overline{\mathcal{B}}(\overline{r}, t) = \mu(t) * \overline{\mathcal{H}}(\overline{r}, t) = \int_{-\infty}^{t} \mu(t - t')\overline{\mathcal{H}}(\overline{r}, t')dt'. \tag{2.22b}$$

Using the Fourier transform pair

$$f(t) = \frac{1}{2\pi}\int_{-\infty}^{+\infty} \widetilde{f}(\omega)e^{+j\omega t}d\omega, \tag{2.23a}$$

$$\widetilde{f}(\omega) = \int_{-\infty}^{+\infty} f(t)e^{-j\omega t}dt, \tag{2.23b}$$

we thus have

$$\widetilde{\overline{\mathcal{D}}}(\overline{r}, \omega) = \widetilde{\varepsilon}(\omega) \cdot \widetilde{\overline{\mathcal{E}}}(\overline{r}, \omega), \tag{2.24a}$$

$$\widetilde{\overline{\mathcal{B}}}(\overline{r}, \omega) = \widetilde{\mu}(\omega) \cdot \widetilde{\overline{\mathcal{H}}}(\overline{r}, \omega). \tag{2.24b}$$

[8]Frequency dispersion in a LH TL medium is clearly apparent in the fundamental relations of Eq. (1.11) and in Fig 1.9(b).

[9]In this section, the notation x/y is a shorthand for "x, respectively, y," and does not mean x divided by y.

[10]We could make the following analogy with road traffic. The flux $\overline{\mathcal{F}}(r, t)$ of vehicles at different points r of a freeway's network as a function of time t depends on the traffic intensity at earlier times $\overline{\mathcal{I}}(r, t')$ $(t' < t)$ weighted by the capacity $c(t)$ of the network to absorb traffic in time: $\overline{\mathcal{F}}(r, t') = \int_{-\infty}^{t} c(t - t')\overline{\mathcal{I}}(r, t')dt'$. If the network had the capacity to absorb traffic instantaneously, the flux of cars at a given time t would depend only on the traffic intensity at the same time, i.e., $c(t) = c\delta(t - t')$, and therefore we would have $\overline{\mathcal{F}}(r, t) = c\overline{\mathcal{I}}(r, t)$. If the network is capable of absorbing traffic very fast, the flux of vehicles is at any time fairly proportional to traffic intensity, $\overline{\mathcal{F}}(r, t) \approx c\overline{\mathcal{I}}(r, t)$; the response of the network is almost instantaneous, and the system is therefore said to be weakly dispersive. If in contrast the network cannot "follow" the traffic intensity, which generally results in a jam, the flux of vehicles strongly depends on the "history" of traffic along the network; we then have a strongly dispersive system, where $c(t')$ is a function exhibiting a slowly decreasing tail for $t' < t$ toward smaller values of t' [with $c(t' > t) = 0$].

Eqs. (2.22) show that, even for time harmonic excitations $\overline{\mathcal{E}}$ and $\overline{\mathcal{H}}$, $\partial/\partial t \neq j\omega$ in a dispersive medium. Therefore, the full time dependence of the different quantities must be retained. The Poynting vector [Eq. (2.19)], expressed in terms of the real fields $\overline{\mathcal{E}}/\overline{\mathcal{H}}$, can then be shown to read as

$$\overline{\mathcal{S}}(\overline{r}, t) = \overline{\mathcal{E}}(\overline{r}, t) \times \overline{\mathcal{H}}(\overline{r}, t). \tag{2.25}$$

This relation is formally identical to (2.19), except for the absence of the complex conjugate "*", which has become meaningless because all fields are now real quantities. The fact that this relation still holds in a dispersive medium can be demonstrated in the following manner. The continuity of the *tangential* components of $\overline{\mathcal{E}}/\overline{\mathcal{H}}$ at the boundary between two media induces the continuity of the *normal* component of $\overline{\mathcal{S}}$ at this interface. Because one of the two media considered can be nondispersive while the other one is assumed dispersive, the normal component of $\overline{\mathcal{S}}$, by continuity, is not affected by dispersion in the dispersive medium. It follows that the tangential components of $\overline{\mathcal{S}}$, although not continuous, are also unaffected by dispersion.[11] Therefore, the expression (2.19) established for a nondispersive medium still holds in the more general case of a dispersive medium, where it is more generally (also for nonharmonic fields) written as Eq. (2.25).

The rate of change of the energy per volume in a body V (see Fig 2.2) is $\nabla \cdot \overline{\mathcal{S}}$. With the use of Eq. (2.25), the sourceless Maxwell's equations (fields considered at locations where no source is present) (2.1a) ($\overline{\mathcal{M}_s} = 0$) and (2.1b) ($\overline{\mathcal{J}_s} = 0$) and the identity $\nabla \cdot (\overline{A} \times \overline{B}) = (\nabla \times \overline{A}) \cdot \overline{B} - (\nabla \times \overline{B}) \cdot \overline{A}$, this quantity becomes

$$\nabla \cdot \overline{\mathcal{S}} = -\left[\overline{\mathcal{E}} \cdot \frac{\partial \overline{\mathcal{D}}}{\partial t} + \overline{\mathcal{H}} \cdot \frac{\partial \overline{\mathcal{B}}}{\partial t}\right]. \tag{2.26}$$

At this point, some kind of assumption on the nature of the fields intensities has to be made in order to derive a useful expression in the frequency domain. Let us therefore consider quasi-harmonic fields with mean frequency ω_0. We can write such fields $\overline{\mathcal{F}}$ (standing for $\overline{\mathcal{E}}$, $\overline{\mathcal{H}}$, $\overline{\mathcal{D}}$ or $\overline{\mathcal{B}}$) in terms of the phasor $\overline{F}$ (standing for $\overline{E}$, $\overline{H}$, $\overline{D}$ or $\overline{B}$) [Eq. (2.4)]

$$\overline{\mathcal{F}} = \mathrm{Re}\left[\overline{F}(t)e^{+j\omega_0 t}\right] = \mathrm{Re}\left[\overline{\mathsf{F}}\right] = \frac{\overline{\mathsf{F}} + \overline{\mathsf{F}}^*}{2}, \quad \left[\overline{\mathsf{F}} = \overline{F}(t)e^{+j\omega_0 t}\right] \tag{2.27}$$

where here $\overline{F}(t)$ is function slowly varying in time in comparison with $e^{+j\omega_0 t}$, so that the field $\overline{\mathcal{F}}$ has a narrow spectrum centered around the mean value of ω_0, and $\overline{\mathsf{F}}$ (standing for $\overline{\mathsf{E}}$, $\overline{\mathsf{H}}$, $\overline{\mathsf{D}}$ or $\overline{\mathsf{B}}$) is the product of the phasor $\overline{F}$ by the harmonic function $e^{+j\omega_0 t}$. Inserting this expression for $\overline{\mathcal{E}}$, $\overline{\mathcal{H}}$, $\overline{\mathcal{D}}$, and $\overline{\mathcal{B}}$ into Eq. (2.26)

[11] Dispersion characteristics are naturally common to all the components of the fields. For instance, in the case of a plane wave, the same dependence $e^{-j\beta(\omega)r}$ is present in all the components.

and noting that the products $\overline{\mathcal{E}} \cdot \partial\overline{\mathcal{D}}/\partial t$, $\overline{\mathcal{E}}^* \cdot \partial\overline{\mathcal{D}}^*/\partial t$, $\overline{\mathcal{H}} \cdot \partial\overline{\mathcal{B}}/\partial t$ and $\overline{\mathcal{H}}^* \cdot \partial\overline{\mathcal{B}}^*/\partial t$ vanish when averaged over time, we obtain

$$\nabla \cdot \overline{\mathcal{S}} = -\frac{1}{4}\left[\overline{\mathsf{E}} \cdot \frac{\partial \overline{\mathsf{D}}^*}{\partial t} + \overline{\mathsf{E}}^* \cdot \frac{\partial \overline{\mathsf{D}}}{\partial t} + \overline{\mathsf{H}} \cdot \frac{\partial \overline{\mathsf{B}}^*}{\partial t} + \overline{\mathsf{H}}^* \cdot \frac{\partial \overline{\mathsf{B}}}{\partial t}\right]. \tag{2.28}$$

To develop the derivatives $\partial\overline{\mathsf{D}}^*/\partial t$, $\partial\overline{\mathsf{D}}/\partial t$, and subsequently $\partial\overline{\mathsf{B}}^*/\partial t$, $\partial\overline{\mathsf{B}}/\partial t$, let us expand $\overline{\mathsf{D}}$ in its Fourier series

$$\begin{aligned}\overline{\mathsf{D}} = \overline{D}(t)e^{+j\omega_0 t} &= \left[\sum_{\omega'} \overline{D}_{\omega'} e^{+j\omega' t}\right] e^{+j\omega_0 t} = \sum_{\omega'} \overline{D}_{\omega'} e^{+j(\omega_0+\omega')t} \\ &= \sum_{\omega'} \varepsilon(\omega_0+\omega')\overline{E}_{\omega'} e^{+j(\omega_0+\omega')t},\end{aligned} \tag{2.29}$$

where we remember that only terms with $\omega' \ll \omega_0$ will subsist in the series due to the assumption of slow time variation of the phasor $\overline{D}$. The derivative of the above expression reads

$$\frac{\partial\overline{\mathsf{D}}}{\partial t} = \sum_{\omega'} f(\omega_0+\omega')\overline{E}_{\omega'} e^{+j(\omega_0+\omega')t}, \quad \text{with} \quad f(\omega) = j\omega\varepsilon(\omega), \tag{2.30}$$

where $f(\omega)$ may be approximated by its Taylor expansion around $\omega = \omega_0$, since $\omega' \ll \omega_0$: $f(\omega) = f(\omega_0) + \left[df(\omega)/d\omega\right]_{\omega=\omega_0}(\omega - \omega_0)$ or $f(\omega_0+\omega') = f(\omega_0) + \dot{f}(\omega_0)\omega'$. We then have

$$\begin{aligned}\frac{\partial\overline{\mathsf{D}}}{\partial t} &= \sum_{\omega'}\left[f(\omega_0)\overline{E}_{\omega'} e^{+j(\omega_0+\omega')t} + \dot{f}(\omega_0)\omega'\overline{E}_{\omega'} e^{+j(\omega_0+\omega')t}\right] \\ &= f(\omega_0)\left[\sum_{\omega'} \overline{E}_{\omega'} e^{+j\omega' t}\right] e^{+j\omega_0 t} + \dot{f}(\omega_0)\left[\sum_{\omega'} \omega'\overline{E}_{\omega'} e^{+j\omega' t}\right] e^{+j\omega_0 t} \\ &= f(\omega_0)\overline{E}e^{+j\omega_0 t} - j\dot{f}(\omega_0)\frac{\partial\overline{E}}{\partial t}e^{+j\omega_0 t} \\ &= f(\omega_0)\overline{\mathsf{E}} - j\dot{f}(\omega_0)\frac{\partial\overline{E}}{\partial t}e^{+j\omega_0 t} \\ &= j\omega_0\varepsilon(\omega_0)\overline{\mathsf{E}} + \left[\frac{d(\omega\varepsilon)}{d\omega}\right]_{\omega=\omega_0}\frac{\partial\overline{E}}{\partial t}e^{+j\omega_0 t}.\end{aligned} \tag{2.31}$$

Omitting henceforward the subscript 0, we have thus for $\partial\overline{\mathsf{D}}/\partial t$

$$\frac{\partial\overline{\mathsf{D}}}{\partial t} = j\omega\varepsilon(\omega)\overline{\mathsf{E}} + \frac{d(\omega\varepsilon)}{d\omega}\frac{\partial\overline{E}}{\partial t}e^{+j\omega t}, \tag{2.32}$$

and similarly for $\partial\overline{\mathsf{B}}/\partial t$

$$\frac{\partial\overline{\mathsf{B}}}{\partial t} = j\omega\mu(\omega)\overline{\mathsf{H}} + \frac{d(\omega\mu)}{d\omega}\frac{\partial\overline{H}}{\partial t}e^{+j\omega t}. \tag{2.33}$$

Substituting these expressions in Eq. (2.28) and neglecting the imaginary parts of $\varepsilon(\omega)$ and $\mu(\omega)$ yields then

$$\begin{aligned}\nabla\cdot\overline{\mathcal{S}} &= -\frac{1}{4}\left\{\frac{d(\omega\varepsilon)}{d\omega}\left[\overline{E}^*\cdot\frac{\partial\overline{E}}{\partial t}+\overline{E}\cdot\frac{\partial\overline{E}^*}{\partial t}\right]+\frac{d(\omega\mu)}{d\omega}\left[\overline{H}^*\cdot\frac{\partial\overline{H}}{\partial t}+\overline{H}\cdot\frac{\partial\overline{H}^*}{\partial t}\right]\right\}\\ &= -\frac{1}{4}\left\{\frac{d(\omega\varepsilon)}{d\omega}\frac{\partial}{\partial t}\left[\overline{\mathsf{E}}\cdot\overline{\mathsf{E}}^*\right]+\frac{d(\omega\mu)}{d\omega}\frac{\partial}{\partial t}\left[\overline{\mathsf{H}}\cdot\overline{\mathsf{H}}^*\right]\right\}\end{aligned} \tag{2.34}$$

since $\overline{\mathsf{E}}\cdot\overline{\mathsf{E}}^* = \overline{E}\cdot\overline{E}^*$ and $\overline{\mathsf{H}}\cdot\overline{\mathsf{H}}^* = \overline{H}\cdot\overline{H}^*$. Rewriting this expression in terms of the real fields $\overline{\mathcal{E}}/\overline{\mathcal{H}}$, we obtain the mean value of the electromagnetic part of the internal energy per unit volume of the medium, $\overline{W} = -\int\nabla\cdot\overline{\mathcal{S}}\,dt$, as[12]

$$\overline{W} = \frac{1}{4}\left[\frac{d(\omega\varepsilon)}{d\omega}\overline{\mathcal{E}^2}+\frac{d(\omega\mu)}{d\omega}\overline{\mathcal{H}^2}\right]. \tag{2.35}$$

If there is no dispersion, ε and μ are constants, and Eq. (2.35) reduces to

$$\overline{W} = \frac{\varepsilon\overline{E^2}+\mu\overline{H^2}}{4}, \tag{2.36}$$

which corresponds, as expected, to the sum $\overline{W} = \overline{W}_e + \overline{W}_m$ of the time average electric and magnetic energies stored in the volume V, where $\overline{W}_e = \varepsilon\overline{\mathcal{E}^2}/4$ and $\overline{W}_m = \mu\overline{\mathcal{H}^2}/4$ according to Eqs. (2.18e) and (2.18f), respectively.

If the external supply of electromagnetic energy to the body is cut off, absorption ultimately converts the energy $\overline{W}$ entirely into heat. By the *law of entropy*, specifying that the entropy of a system is an ever increasing quantity, there must be evolution and not absorption of heat [3]. We therefore must have

$$\overline{W} > 0, \tag{2.37}$$

which leads in the general (dispersive) case to the inequalities

$$\frac{d(\omega\varepsilon)}{d\omega} > 0, \tag{2.38a}$$

$$\frac{d(\omega\mu)}{d\omega} > 0, \tag{2.38b}$$

[12]It should be kept in mind that this relation is valid only for fields whose amplitude varies sufficiently slowly with time in comparison with $e^{+j\omega_0 t}$.

since $\overline{\mathcal{E}^2} > 0$ and $\overline{\mathcal{H}^2} > 0$. Eq. (2.37) is called the *entropy condition*, which is seen to be different in the general case of a dispersive medium [Eq. (2.35)] than in the particular case of a nondispersive medium [Eq. (2.36)].[13] Eqs. (2.38) are the *general entropy conditions for the constitutive parameters*. These entropy conditions show that *simultaneously negative ε and μ are physically impossible in a nondispersive medium* since they would violate the law of entropy. They also show that, in contrast *in a dispersive medium, simultaneously negative ε and μ are allowed*, as long as the frequency dependent ε and μ satisfy the conditions of Eqs. (2.38). For this to be achieved, ε and μ must be positive in some parts of their spectrum, to compensate for the negative parts, which shows that a LH medium is necessarily dispersive.

2.3 BOUNDARY CONDITIONS

The boundary conditions (BCs) at the interface between two media, which are directly derived from Maxwell equations and therefore clearly hold also in the case of LH media, read

$$\hat{n} \cdot (\overline{D}_2 - \overline{D}_1) = \rho_{es}, \tag{2.39a}$$

$$\hat{n} \cdot (\overline{B}_2 - \overline{B}_1) = \rho_{ms}, \tag{2.39b}$$

$$\hat{n} \times (\overline{E}_2 - \overline{E}_1) = -\overline{M}_s, \tag{2.39c}$$

$$\hat{n} \times (\overline{H}_2 - \overline{H}_1) = \overline{J}_s, \tag{2.39d}$$

where ρ_{se} is the electric surface charge density on the interface, ρ_{sm} is the magnetic (fictitious) surface charge density on the interface, and $\hat{n}$ is a unit vector normal to the interface pointing from medium 1 to medium 2. The first two equations of (2.39) state that, in the absence of charges ($\rho_{es} = \rho_{em} = 0$) at the interface, the normal components of $\overline{D}$ and $\overline{B}$ are continuous, whereas the last two questions of (2.39) state that, in the absence of sources ($\overline{J}_s = \overline{M}_s = 0$) at the interface, the normal tangential components of $\overline{E}$ and $\overline{H}$ are continuous, i.e.,

$$D_{1n} = D_{2n}, \tag{2.40a}$$

$$B_{1n} = B_{2n}, \tag{2.40b}$$

$$E_{1t} = E_{2t}, \tag{2.40c}$$

$$H_{1t} = H_{2t}, \tag{2.40d}$$

where the indexes n and t stand for normal and tangential, respectively.

Let us consider now the specific case of an interface between a RH and a LH media, illustrated in Fig 2.3 (medium 1: LH, medium 2: RH). The relations of

[13] In a nondispersive medium, the entropy conditions simply read $\varepsilon > 0$ and $\mu > 0$.

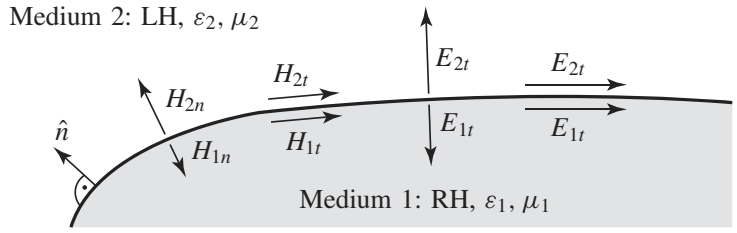

Fig. 2.3. Boundary conditions at the interface between a RH medium and a LH medium.

Eqs. (2.40) reveal the following. The BCs on the tangential components of $\overline{E}/\overline{H}$ are unaffected at this interface, since the relations on the tangential components do not depend on ε, μ. In contrast, the BCs on the normal components are necessarily changed, since they involve ε, μ with changes in signs. By assuming that the LH medium is weakly dispersive and that therefore the constitutive relations (2.2) or (2.6) are approximately valid, we obtain the following BCs at a RH/LH interface:

$$E_{1n} = -\frac{\varepsilon_2}{|\varepsilon_1|} E_{2n}, \tag{2.41a}$$

$$H_{1n} = -\frac{\mu_2}{|\mu_1|} H_{2n}, \tag{2.41b}$$

$$E_{1t} = E_{2t}, \tag{2.41c}$$

$$H_{1t} = H_{2t}. \tag{2.41d}$$

Thus *the tangential components of* $\overline{E}/\overline{H}$ *remain continuous while their normal components become antiparallel* at the interface between a RH medium and a LH medium. The BCs on the normal components of $\overline{E}/\overline{H}$ can be written in general, for and interface between arbitrary RH-LH media, as follows:

$$E_{1n} = s_1 s_2 \frac{|\varepsilon_2|}{|\varepsilon_1|} E_{2n}, \tag{2.42a}$$

$$H_{1n} = s_1 s_2 \frac{|\mu_2|}{|\mu_1|} H_{2n}, \tag{2.42b}$$

where s_i $(i = 1, 2)$ represents the sign of handedness of the medium i, as defined in Eq. (2.13).

2.4 REVERSAL OF DOPPLER EFFECT

Consider a source S in motion along a direction z and radiating omnidirectionally an electromagnetic wave with angular frequency ω, as illustrated in Fig 2.4. In

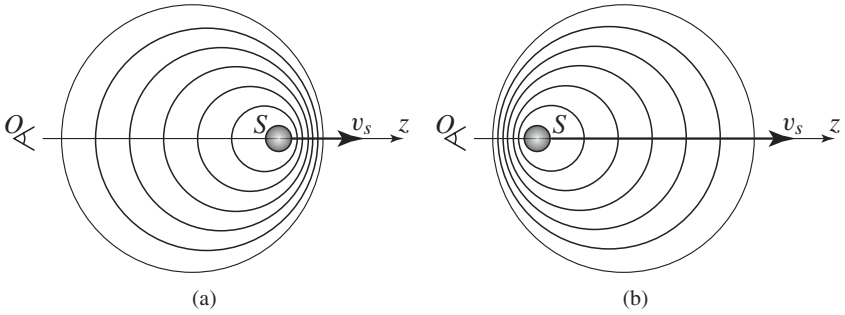

Fig. 2.4. Doppler effect. (a) Conventional, in a RH medium ($\Delta\omega > 0$). (b) Reversed, in a LH medium ($\Delta\omega < 0$).

the far-field of the source,[14] the radiated fields have the form [4]

$$\overline{\mathsf{E}}(z,t), \overline{\mathsf{H}}(z,t) \propto \frac{e^{j\varphi(\omega,t)}}{r}, \quad \text{with} \quad \varphi(\omega,t) = \omega t - \beta r, \tag{2.43}$$

where β represents the wave number in the medium in which S moves and radiates and r the standard radial variable of the spherical coordinates system.

Let us consider what happens to the radiated wave along the direction of the motion of the source, i.e., for $r = z$ (in $\theta = 0$). If the sources moves toward positive values of z with a velocity $v_s = z/t$, its position as a function of time is $z = v_s t$. Consequently, the phase seen by an observer O located at the left-hand side of S (i.e., looking at S toward positive values of z) may be developed as follows along the z axis:

$$\varphi = \omega t - \beta v_s t = \omega\left(1 - \frac{\beta}{\omega}v_s\right)t = \omega\left(1 - \frac{v_s}{v_p}\right)t = \omega\left(1 - s\frac{v_s}{|v_p|}\right)t, \tag{2.44}$$

since $\omega/\beta = v_p$ according to Eq. (2.10). The coefficient of t is the Doppler frequency ω_{Doppler}, which is the difference of the frequency ω of the motionless ($v_s = 0$) source and the Doppler frequency shift $\Delta\omega$,

$$\omega_{\text{Doppler}} = \omega - \Delta\omega, \quad \text{with} \quad \Delta\omega = s\frac{v_s}{|v_p|}, \tag{2.45}$$

where s is the handedness sign function defined in Eq. (2.13). In a RH medium, $\Delta\omega > 0$ since $s = +1$, and therefore the frequency measured by the observer looking at the receding source is shifted downward or "red-shifted," as illustrated in Fig 2.4(a); on the other hand, an observer located on the right-hand side of the source, i.e., seeing a proceeding source, would measure a frequency shifted upward or "blue-shifted," because the sign of v_s would be changed for that observer [6]. In a LH medium, because $s = -1$, the whole phenomenon is

[14]The far-field region is defined as $r > 2D^2/\lambda$, where D is the largest size of the source (antenna) [4].

reversed, as shown in Fig 2.4(b): The Doppler frequency of a receding source is blue-shifted, whereas that of a proceeding source is red-shifted. This phenomenon of reversal of Doppler effect in a LH medium was pointed out by Veselago back in 1967 as an immediate consequence of left-handedness [5] (Section 1.2).

2.5 REVERSAL OF VAVILOV-ČERENKOV RADIATION

In his paper [5], Veselago also pointed out that a LH medium would induce reversal of Vavilov-Čerenkov radiation (Section 1.2). Vavilov-Čerenkov radiation is the visible electromagnetic radiation emitted by liquids and solids when bombarded by fast-moving electron beams with high velocity. For simplicity, let us consider a single electron $e-$ of charge q moving at the velocity v_e along a direction z, as illustrated in Fig 2.5. The current density for this charge is

$$\overline{\mathcal{J}}(\overline{r}, t) = \hat{z} q v_e \delta(x)\delta(y)\delta(z - v_e t), \tag{2.46}$$

where $\hat{z}$ is a unit vector directed along the direction z. By solving the wave equation for this source in the cylindrical coordinate system, one obtains the electric field intensity solution [7]

$$\begin{aligned} \overline{E}(\overline{r}) &= -\frac{q}{8\pi\omega\varepsilon}\left[\hat{z}k^2 - j\frac{\omega}{v_e}\nabla\right] H_0^{(1)}(k_\rho \rho) e^{-j\omega z/v_e} \\ &\overset{k_\rho\rho \gg 1}{=} -\frac{q}{8\pi\omega\varepsilon}\sqrt{\frac{2jk_\rho}{\pi\rho}}\left[\hat{\rho}\frac{\omega}{v_e} - \hat{z}k_\rho\right] e^{-j(k_\rho\rho + \omega z/v_e)}, \end{aligned} \tag{2.47a}$$

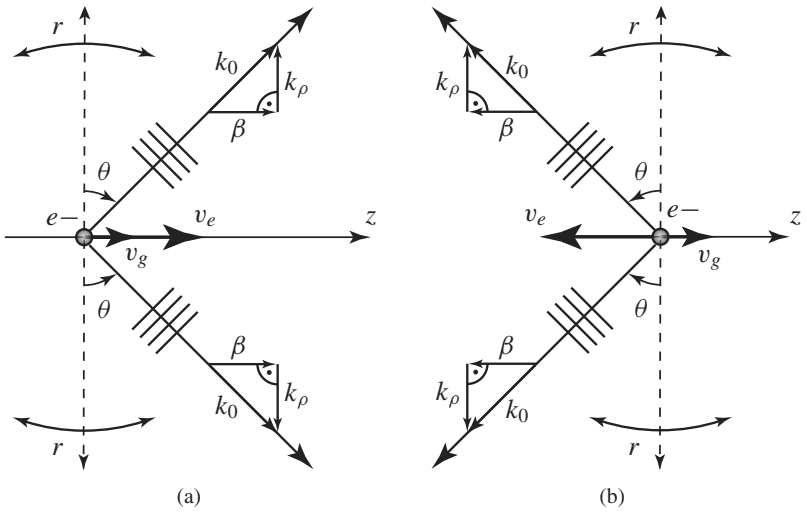

Fig. 2.5. Vavilov-Čerenkov radiation. v_g would represent the group velocity of the beam including the electron. (a) Conventional, in a RH medium ($\theta > 0$). (b) Reversed, in a LH medium ($\theta < 0$).

where

$$k_\rho = \sqrt{k^2 - \beta^2}, \quad \text{with} \quad \beta = \frac{\omega}{v_e}. \tag{2.47b}$$

Due to its wave nature, "the isolated electron considered *is* the wave" and therefore the phase velocity $v_p = \omega/\beta$ of the wave along z is the same thing as the velocity of the electron, $v_p = v_e$. This is the reason why we have $\beta = \omega/v_e$ in the above relations.[15]

It is worth noting that the phenomenon of Vavilov-Čerenkov radiation is fundamentally similar to the phenomenon of leakage radiation in traveling-wave antennas (Section 6.1). The link between the two descriptions may be understood by considering the fact that a beam of electrons in motion is equivalent to an electric current ($i = dq/dt$). From this point of view, a transmission line supporting a fast-wave ($v_p > c$) (leaky-wave structure) is equivalent to a transmission medium supporting a beam of fast-wave electrons ($v_e > c$). This analogy can be further extended to an array of antennas [4] where the phase difference $\varphi = -\beta p$ between the elements (separated by a distance p) may be considered equivalent to a wave propagating along the array with the velocity $v_p = \omega/\beta$ [8].

Examination of Eq. (2.47) explains the phenomena observed by Čerenkov in his experiments [7]:

- Since radiation requires $k_\rho \in \mathbb{R}$ (propagation along the direction perpendicular to the direction of motion of the beam), radiation can occur only in the frequency range where $k > \beta = \omega/v_e$, i.e., $v_e > \omega/k = c$. Thus, radiation occurs only at frequencies where the velocity of the electrons is larger than the speed of light. If $v_e < c$, k_ρ is imaginary, and therefore exponential decay of the fields occurs in the direction perpendicularly to the beam. In the leaky-wave approach, the dispersion or $\omega - \beta$ diagram is plotted along with the air lines $\omega = \pm k_0 c$, delimiting the "radiation cone" (Section 6.1). When the structure is excited at a point (ω, β) of the dispersion lying inside this cone, the wave in the direction of the line is called a *fast wave*, because $v_p > c$, and leakage radiation occurs; when the structure is excited at a point lying outside this region, the wave is called a *slow wave*, because $v_p < c$, and the wave is purely guided along the line, without radiation.
- Vavilov-Čerenkov radiation is directive, with a radiation angle depending on the velocity of the electrons. This radiation angl can be straightforwardly

[15]This fact is the most essential distinction between the Doppler "event" (Section 2.4) and the Vavilov-Čerenkov "event." In the case of the Doppler effect, the source in motion considered is not a relativistic particle, such as an electron, but macroscopic object (e.g., an antenna), the velocity (of motion) of which, v_s, has no relation with the phase velocity v_p of the wave it radiates ($v_p \neq v_e$). Otherwise, the Doppler effect and the Vavilov-Čerenkov radiation would be the same phenomenon! Another fundamental difference is that, in the case of Vavilov-Čerenkov, radiation occurs only if the source velocity is larger than the velocity of light, $v_e = v_p > c$ (fast-wave), whereas in the case of Doppler, radiation is a mechanism totally independent from the motion of the object, which can therefore occur for any source velocity v_s.

determined with the help of Fig 2.5(a)

$$\theta = \sin^{-1}\left(\frac{\beta}{k_0}\right) = \sin^{-1}\left(\frac{c}{v_e}\right). \tag{2.48}$$

It is clear in this relation that, if $v_e < c$, the angle θ is imaginary, consistent with the fact that there is no radiation in this case. This relation is exactly identical to that used in leaky-wave antennas (Section 6.1, Eq. 6.3).

- With regard to the polarization, $\overline{E}$ lies in the plane determined by $\overline{k}$ and $\hat{z}$. In addition, we have $\overline{E} \perp \overline{k}_0$ since $\overline{k}_0 \cdot \overline{E} = 0$. The following intuitive explanation is provided in [7] to explain this polarization. When the charged particle is at rest, the electric field points radially, whereas when the particle moves the field lines are bent at an angle proportional to the velocity of the particle, eventually breaking away from the charge to produce radiation when $v_e > c$.

From the above explanations and in particular Eq. (2.48), it is obvious that, in a RH medium, Vavilov-Čerenkov radiation occurs at positive θ angles (in the half-plane in the direction of motion of the particle), since $\beta > 0$, as shown in Fig 2.5(a). If in contrast the medium is LH, $\beta < 0$, radiation occurs at negative θ angles (in fact also the half-plane in the direction of motion of the particle but opposite to the group velocity of the beam including it). To better understand the meaning of this reversal of Vavilov-Čerenkov radiation, a source generating a modulated beam of electrons should be considered. In this case, if the source emits electrons toward positive values of z, power (v_g) would naturally propagate toward positive z, whereas the electron wave would propagate backward in the LH medium.

A theoretical study of Vavilov-Čerenkov radiation in a LH medium is presented in [9]. The conclusions of this paper correspond point by point to those obtained for the CRLH backfire-to-endfire leaky-wave antenna, which will be presented in Section 6.2.

2.6 REVERSAL OF SNELL'S LAW: NEGATIVE REFRACTION

One of the most remarkable property of LH media is their negative refractive index (NRI), already demonstrated in Section 2.1. In this section, we will show the consequences of NRI when the LH medium is interfaced with a RH medium.

Let us consider the classical problem of a plane wave incident upon the boundary between two homogeneous media, illustrated in Fig 2.6. In general, from the incident wave, $e^{-j\overline{k_i}\cdot\overline{r}}$, in medium 1, a reflected wave, $e^{-j\overline{k_r}\cdot\overline{r}}$, in medium 1, and a transmitted (or refracted) wave in medium 2, $e^{-j\overline{k_t}\cdot\overline{r}}$, are generated. The boundary condition [Eq. (2.41)] requires that the tangential components of $\overline{E}$ and $\overline{H}$ be continuous at $z = 0$ for all x and y. Calling the magnitudes of the

tangential incident, reflected, and transmitted electric field[16] $E_{i,tan}$, $E_{r,tan}$ and $E_{t,tan}$, respectively, we must have (at $z = 0$) in all possible cases

$$E_{i,tan}e^{-j(k_{ix}x+k_{iy}y)} + E_{r,tan}e^{-j(k_{rx}x+k_{ry}y)} = E_{t,tan}e^{-j(k_{tx}x+k_{ty}y)}, \tag{2.49}$$

since the total field is the sum of the incident and reflected field in medium 1 and the transmitted field in medium 2. The only way that this equation can be satisfied for all x and y (of the interface) is to have $E_{i,tan} + E_{r,tan} = E_{t,tan}$, and therefore

$$k_{ix} = k_{rx} = k_{tx} = k_x, \tag{2.50a}$$

$$k_{iy} = k_{ry} = k_{ty} = k_y, \tag{2.50b}$$

which show that the tangential component of the wave number $\overline{k}_{tan} = k_x\hat{x} + k_y\hat{y}$ is continuous at the interface between two media

$$\overline{k}_{1,tan} = \overline{k}_{2,tan}. \tag{2.51}$$

This relation is the *phase matching-condition*, which is a direct consequence of the continuity of the tangential components of $\overline{E}$ and $\overline{H}$ and which also holds at the interface between a RH medium and a LH medium since the continuity of $\overline{E}$ and $\overline{H}$ is conserved in this case (Section 2.3). Another information provided by the phase matching condition is that the incident, reflected, and transmitted wave vectors must all lie in the *plane of incidence*, which is the plane determined by $\overline{k}_i$ and the normal to the interface (z axis).

The tangential components of the wave numbers can be expressed as a function of their corresponding angle with the help of Fig 2.6. For instance, for the x components we have

$$k_{ix} = k_i \sin\theta_i, \quad k_{rx} = k_r \sin\theta_r, \quad k_{tx} = k_t \sin\theta_t, \tag{2.52}$$

where the wave numbers are

$$k_i = \frac{\omega\sqrt{\varepsilon_{r1}\mu_{r1}}}{c} = \frac{\omega n_1}{c} = k_r = k_1, \quad k_t = \frac{\omega\sqrt{\varepsilon_{r2}\mu_{r2}}}{c} = \frac{\omega n_2}{c} = k_2. \tag{2.53}$$

Eqs. (2.51) and (2.52) applied to the incident and reflected waves lead to the relation $k_i \sin\theta_i = k_r \sin\theta_r$, which, with Eq. (2.53), yields *Snell's law of reflection*

$$\theta_r = \theta_i. \tag{2.54}$$

This law is unchanged at the interface between a RH medium and a LH medium, because it relates fields in the same medium. Eqs. (2.51) and (2.52)

[16]Of course, the magnetic field can also be considered instead of the electric field.

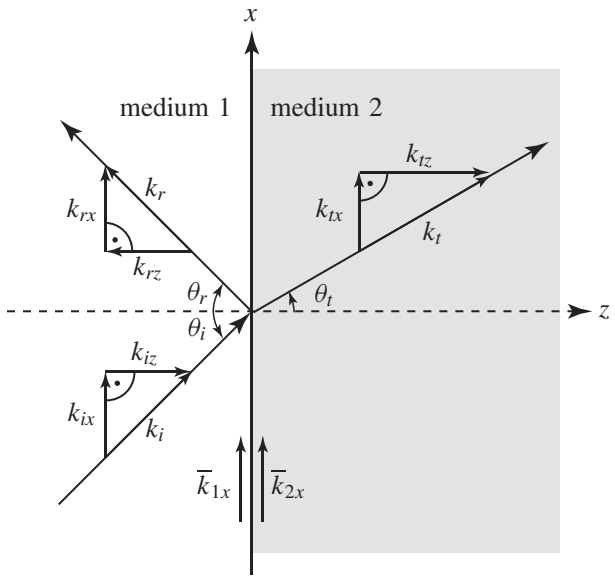

Fig. 2.6. Phase-matching at the boundary between two media. The angles θ_i, θ_r, and θ_t are the incident, reflected, and transmitted (or refracted) angles, respectively.

applied to the incident and transmitted waves lead to the relation $k_i \sin\theta_i = k_t \sin\theta_t$, which, with Eq. (2.53), yields *Snell's law of refraction*

$$n_1 \sin\theta_1 = n_2 \sin\theta_2. \tag{2.55}$$

This law is modified at the interface between a RH medium and a LH medium, due to the apparition of a negative sign in the refractive index of the LH medium (Section 2.1). Snell's law of refraction may be written in the more general form

$$s_1|n_1| \sin\theta_1 = s_2|n_2| \sin\theta_2, \tag{2.56}$$

where it also appears that if the two media are LH, Snell's law is unchanged due to mutual cancelation of the two minus signs of the two refractive indexes. Form (2.56), the reversal of Snell's law at the interface between a RH medium and a LH medium, illustrated in Fig 2.7, is manifest. A wave incident upon the interface between two media with same handedness (e.g., RH) experiences conventional *positive refraction*, characterized by a positive[17] refraction angle [Fig 2.7(a)], whereas a ray at the interface between two media of different handednesses (RH and LH) undergoes *negative refraction*, corresponding to negative refraction angle or NRI [Fig 2.7(b)].

[17]This is based on the convention that positive angles correspond to the counter-clockwise direction or rotation.

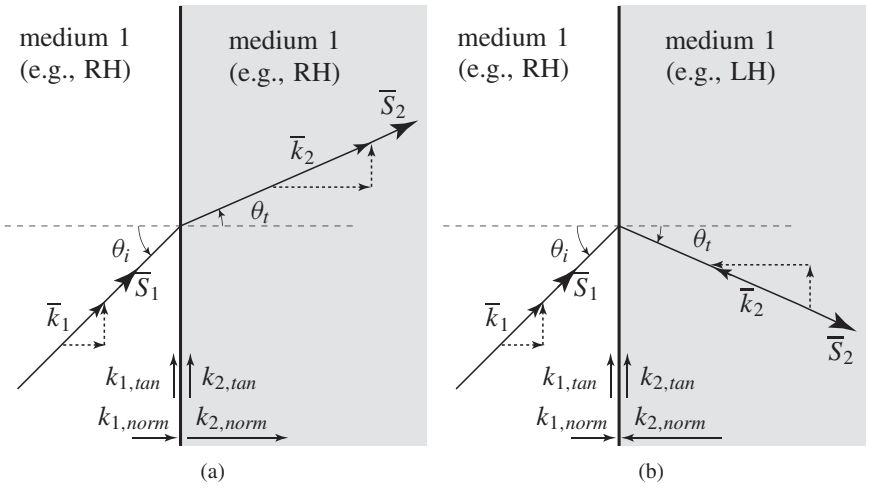

Fig. 2.7. Refraction of an electromagnetic wave at the interface between two different media. (a) Case of two media of same handedness (either RH or LH): positive refraction. (b) Case of two media of different handedness (one RH and the other one LH): negative refraction.

As a consequence of phase matching [Eq. (2.51)] and of the sign of the refractive index [Eq. (2.17)] in each of the two media, it is immediately apparent in Fig 2.7, that although the normal components of the wave vector $\overline{k}_{norm}$ are parallel at a RH/RH or LH/LH interface they are antiparallel at a RH/LH interface. The relation between the normal components of the wave vectors at the interface may be written in the general form

$$s_1|n_1| \cdot |\overline{k}_{2,norm}| = s_2|n_2| \cdot |\overline{k}_{1,norm}|. \tag{2.57}$$

Fig 2.7 also shows the Poynting vectors $\overline{S}_i$ which, according to Section 2.1, are parallel and antiparallel to the wave vector in RH medium and LH medium, respectively.

Various NRI effects will be illustrated by full-wave simulated fields distributions in Section 4.4, including the focusing effect induced by a flat lens, which is presented in the following section.

2.7 FOCUSING BY A "FLAT LH LENS"

By applying Snell's law [Eq. (2.56)] twice to a LH slab sandwiched between two RH media, also called a LH "lens,"[18] we obtain the *double focusing effect*

[18]This structure, although producing focusing, is not stricto senso a lens, considering that in principle a lens transforms a spherical wave into a plane wave, or vice versa, and not into another spherical wave, as it is the case for the LH slab.

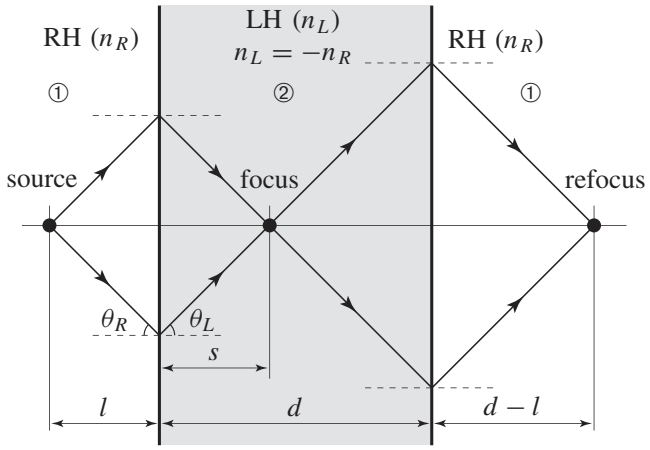

Fig. 2.8. Double focusing effect in a "flat lens," which is a LH slab of thickness d and refractive index n_L sandwiched between two RH media of refractive index n_R with $n_L = -n_R$.

depicted in Fig 2.8[19] [5]: two radiated rays with equal symmetric angles from a source at the distance l from the first interface are negatively refracted under an angle of same magnitude to meet at a distance s in the slab; then they focus again after a second negative refraction in the second RH medium at the distance $d - l$ from the second interface, where s is obtained by simple trigonometric considerations as

$$s = l \frac{\tan \theta_R}{\tan |\theta_L|}, \tag{2.58}$$

where the angle θ_R is the incidence angle and θ_L is obtained by Snell's law [Eq. (2.56)], $\theta_L = -\sin^{-1}\left[(n_R/n_L)\sin\theta_R\right]$. Formula (2.58) shows that if the two media have the same *electromagnetic density*, that is, refractive indexes of same magnitude ($n_L = -n_R$), focus is obtained at the mirror image of the source, $s = l$, since $|\theta_L| = \theta_R$ from Snell's law.

Let us now, instead of two isolated symmetric plane waves (Fig 2.8), consider a collection of plane waves (or rays), or more generally a cylindrical (2D problem) or spherical (3D problem) electromagnetic wave, as typically radiated by a point source. It is then necessary to have the two media with the same electromagnetic density to achieve good focusing. In this case, each pair l of symmetric rays with incidence angle $\theta_{R,l}$ focus at the same point, because $\theta_{L,l} = \theta_{R,l}$, $\forall l$, so that

[19]The motivation for using a slab with double interface, as opposed to single interface, for focusing is that it is assumed that the electromagnetic waves cannot be detected and manipulated *inside* the LH material but only in the air regions, as in the case of a conventional optical lens. However, this assumption is not necessarily pertinent in microwaves, as one could envision to detect and utilize a wave focused inside the LH structure.

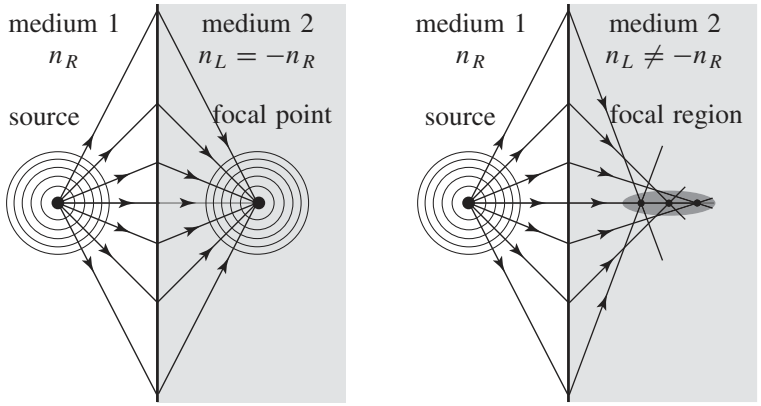

Fig. 2.9. Problem of spherical aberration. (a) When the two media have the same electromagnetic density $n_L = -n_R$, a pure focal point is formed. (b) When the two media have different electromagnetic densities $n_L \neq -n_R$, spherical aberration occurs.

the focal distances are the same for all pairs of rays, $s_l = s \ \forall m$, according to Eq. (2.58), as illustrated in Fig 2.9(a). If the electromagnetic densities of the two media are different ($|n_L| \neq n_R$), then rays with different incidence angles refract to different focal points because the ratios $\tan\theta_{R,l}/\tan|\theta_{L,l}|$ of the different pairs of rays are all different, leading to different focal distances s_l. In that case, *spherical aberration* [11], illustrated in Fig 2.9(a), occurs, and the focal point degenerates into a diffuse focal spot with area increasing with the contrast of refractive indexes, $|n_L|/n_R$

2.8 FRESNEL COEFFICIENTS

In this section, we will see how Fresnel coefficients (reflection coefficient R and transmission coefficient T) at an interface between two arbitrary media are affected when one of the two media is LH. For simplicity, we restrict ourselves to the case of loss-less media [i.e., with zero imaginary parts of their constitutive parameters, according to Eq. (2.3)]. The reflection and transmission coefficients for parallel polarization ($\overline{E}$ parallel to the plane of incidence, also called E, TM_z, p) and perpendicular polarization ($\overline{E}$ perpendicular to the plane of incidence, also called H, TE_z, s) are given, with reference to Fig 2.6, by [10]

$$R_{\parallel} = \frac{\varepsilon_{r1}k_{2z} - \varepsilon_{r2}k_{1z}}{\varepsilon_{r1}k_{2z} + \varepsilon_{r2}k_{1z}} = \frac{\eta_2\cos\theta_2 - \eta_1\cos\theta_1}{\eta_2\cos\theta_2 + \eta_1\cos\theta_1}, \tag{2.59a}$$

$$T_{\parallel} = \frac{2(\varepsilon_{r1}\varepsilon_{r2}\mu_{r2}/\mu_{r1})k_{1z}}{\varepsilon_{r1}k_{2z} + \varepsilon_{r2}k_{1z}} = \frac{2\eta_2\cos\theta_1}{\eta_2\cos\theta_2 + \eta_1\cos\theta_1}, \tag{2.59b}$$

$$R_\perp = \frac{\mu_{r2}k_{1z} - \mu_{r1}k_{2z}}{\mu_{r2}k_{1z} + \mu_{r1}k_{2z}} = \frac{\eta_2 \cos\theta_1 - \eta_1 \cos\theta_2}{\eta_2 \cos\theta_1 + \eta_1 \cos\theta_2}, \tag{2.59c}$$

$$T_\perp = \frac{2\mu_{r2}k_{1z}}{\mu_{r2}k_{1z} + \mu_{r1}k_{2z}} = \frac{2\eta_2 \cos\theta_1}{\eta_2 \cos\theta_1 + \eta_1 \cos\theta_2}, \tag{2.59d}$$

where η_i $(i = 1, 2)$ is the intrinsic impedance of medium i $(i = 1, 2)$

$$\eta_i = \sqrt{\frac{\mu_i}{\varepsilon_i}}. \tag{2.60}$$

These formulas, by setting $k_{z2} = -|k_{z2}|$ [Fig 2.7(b)], $\varepsilon_{r2} = -|\varepsilon_{r2}|$, and $\mu_{r2} = -|\mu_{r2}|$, show that *the Fresnel coefficients at a RH/LH interface are equal in magnitude to the Fresnel coefficients at a RH/RH interface*. The reason for conservation of the *magnitude* of the Fresnel coefficients is that these coefficients depend only on the tangential components of the fields, which are unchanged from a RH/RH interface to a RH/LH interface, as shown in Eqs. (2.41c) and (2.41d). In addition, *the Fresnel coefficients at a RH/LH interface are also equal in phase to the Fresnel coefficients at a RH/RH interface, except for the transmission coefficient for parallel polarization $T_\parallel$, the phase of which is reversed*.[20]

Whereas the indexes of refraction (2.17), related to the product of the permittivity and the permeability, determine the angle of transmission by Snell's law, the intrinsic impedances (2.60), related to the ratio of the permeability to the permittivity, determine the amount of reflection and transmission. Fresnel coefficients are therefore matching parameters, which are of particular importance in microwave and millimeter-wave structures. This observation emphasizes the following fact for the LH slab of Section 2.7 (Fig 2.8). In order to have "perfect" focusing, we must use a LH slab not only with the same refractive index as the index of the sandwiching RH media, to avoid spherical aberration, but also with the same intrinsic impedance, to obtain perfect transmission without reflection, as seen in Eq. (2.59) (where $\theta_1 = \theta_2$ for all pairs of symmetric rays if $|n_2| = n_1$). This means that we must have both same products and same ratios of permittivity and permeability and we therefore must have

$$\varepsilon_1 = \varepsilon_2, \tag{2.61a}$$

and

$$\mu_1 = \mu_2, \tag{2.61b}$$

which obviously represents a much more important design constraint than the isolated condition $n_2 = -n_1$. This is one of the reasons why focusing by a flat lens (Section 2.7) is relatively difficult to achieve.

[20]Note that it would be the phase of the transmission coefficient for *perpendicular* polarization $T_\perp$ that would be reversed in the complementary configuration of a RH slab in a LH environment.

2.9 REVERSAL OF GOOS-HÄNCHEN EFFECT

The Goos-Hänchen effect is the displacement d of a beam of light, or more generally of an electromagnetic wave, impinging on a planar interface with an optically rarer dielectric material under an angle where total reflection occurs. This phenomenon was first conjectured by Newton [14] and later demonstrated experimentally by Goos and Hänchen [15].

Let us rewrite the reflection coefficients given in Section 2.8 in the form

$$R_{\parallel} = \frac{1 - (\varepsilon_{r2}/\varepsilon_{r1})(k_{1z}/k_{2z})}{1 + (\varepsilon_{r2}/\varepsilon_{r1})(k_{1z}/k_{2z})}, \tag{2.62a}$$

$$R_{\perp} = -\frac{1 - (\mu_{r2}/\mu_{r1})(k_{1z}/k_{2z})}{1 + (\mu_{r2}/\mu_{r1})(k_{1z}/k_{2z})}, \tag{2.62b}$$

which is more tractable for the argument of this section. In the Goos-Hänchen effect, the incidence medium (medium 1) is rarer (has smaller electromagnetic density or magnitude of refractive index) than the medium with which it is interfaced (medium 2) (i.e., $n_1 > n_2$) and the incidence angle is larger than the critical angle ($\theta_i > \theta_c > \sin^{-1}|n_2/n_1|$), so that *total internal reflection* occurs. In this case, the normal component of the wave vector is real in the incidence medium and imaginary in the other medium[21]

$$k_{1z} = p_1 = \sqrt{n_1 k_0^2 - k_x^2}, \tag{2.63a}$$

$$k_{2z} = -jq_2 = -j\sqrt{k_x^2 - n_2 k_0^2}, \tag{2.63b}$$

where x is a variable along the plane of the interface, $p_1 \in \mathbb{R}$, $p_1 > 0$, assuming that medium 1 is RH, to ensure outgoing propagation away from the source, and $q_2 \in \mathbb{R}$, $q_2 > 0$ to ensure exponential decay away form the source. With these relations, the reflection coefficients (2.62) may be written in polar form as [16]

$$R_{\parallel} = |R_{\parallel}|e^{j\varphi_{\parallel}} \quad \text{with} \quad \varphi_{\parallel} = -2\tan^{-1}\left(\frac{\varepsilon_{r2}}{\varepsilon_{r1}}\frac{p_1}{q_2}\right) = -2\tan^{-1}(\xi_{\parallel}), \tag{2.64a}$$

$$R_{\perp} = |R_{\perp}|e^{j\varphi_{\perp}} \quad \text{with} \quad \varphi_{\perp} = \pi - 2\tan^{-1}\left(\frac{\mu_{r2}}{\mu_{r1}}\frac{p_1}{q_2}\right) = \pi - 2\tan^{-1}(\xi_{\perp}), \tag{2.64b}$$

where p_1, q_2 in $\varphi_{\parallel}$ and $\varphi_{\perp}$ are functions of k_x via Eq. (2.63). The Goos-Hänchen shifts can be computed from these relations as

$$d_{\parallel} = -\frac{\partial\varphi_{\parallel}}{\partial k_x} = -\frac{2}{1+\xi_{\parallel}^2}\frac{\varepsilon_{r2}}{\varepsilon_{r1}}\frac{k_x}{p_1 q_2}\left[1 - \left(\frac{p_1}{q_2}\right)^2\right], \tag{2.65a}$$

[21]The two media are assumed here to be loss-less for simplicity.

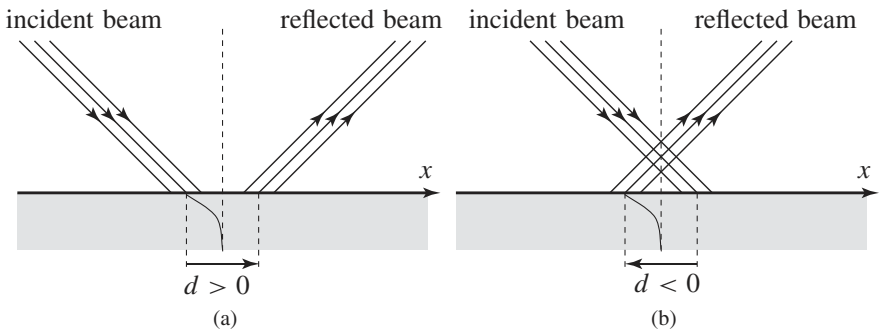

Fig. 2.10. Goos-Hänchen effect. (a) Conventional case, at the interface between two RH media. (b) Reversed effect, at the interface between a RH medium and a LH medium.

$$d_\perp = -\frac{\partial \varphi_\perp}{\partial k_x} = -\frac{2}{1+\xi_\perp^2}\frac{\mu_{r2}}{\mu_{r1}}\frac{k_x}{p_1 q_2}\left[1-\left(\frac{p_1}{q_2}\right)^2\right], \tag{2.65b}$$

where, according to (2.63),

$$\left(\frac{p_1}{q_2}\right)^2 = \frac{n_1 k_0^2 - k_x^2}{k_x^2 - n_2 k_0^2} > 0, \tag{2.66}$$

since $p_1, q_2 \in \mathbb{R}$ and $p_1, q_2 > 0$. These relations with Eq. (2.64) reveal the following phenomenon. If both media are RH, $p_1/q_2 > 1$ since $n_1, n_2 > 0$ and $n_1 > n_2$, so that $d_\parallel$ and $d_\perp$ are positive quantities (i.e., with the same sign as k_x), according to Eq. (2.65). This corresponds to the positive shift of the beam observed by Goos and Hänchen, which is depicted in Fig 2.10(a).

If in contrast, medium 2 is replaced by a LH medium, the signs of ε_{r2} and μ_{r2} are reversed. Consequently, for parameters still satisfying the inequality of Eq. (2.66) after n_2 has been replaced by $-|n_2|$, negative phase shifts are obtained for $d_\parallel$ and $d_\perp$, as illustrated in Fig 2.10(b). Thus the Goos-Hänchen effect has been reversed [16, 17]. It should be noted that for parallel polarization medium 2 does not need to be LH but may only have negative permittivity (and positive permeability) and that, similarly, for parallel polarization medium 2 does not need to be LH but may only have negative permeability (and positive permittivity).

Goos-Hänchen shifts occurring in *layered structures* with negative refraction were analyzed by Shadrivov et al. in [18].

2.10 REVERSAL OF CONVERGENCE AND DIVERGENCE IN CONVEX AND CONCAVE LENSES

Due to their effectively homogeneous nature, in the frequency range of interest, MTMs represent a new paradigm to perform "conventional optics in non conventional materials at microwave frequencies," where in principle simple *ray*

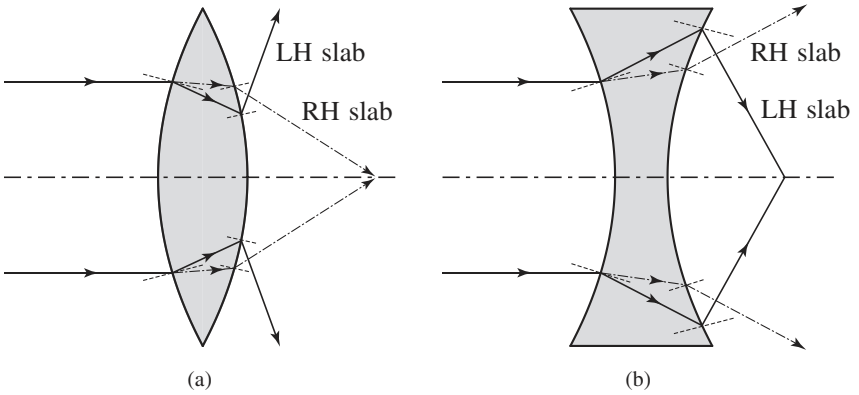

Fig. 2.11. Convergence and divergence induced by RH and LH (curved) lenses in air. (a) A LH convex lens is diverging, whereas a RH convex lens is converging. (b) A LH concave lens is converging, whereas a RH concave lens is diverging.

optics laws directly apply [11], as already shown in Sections 2.6, 2.7, 2.8, and 2.9. In practice, a typical limitation could be the too large electrical size of the unit cell p/λ_g at frequencies too far from the phase origin, where $p/\lambda_g = 0$[22] (Section 1.8). At those frequencies, some amount of diffraction or scattering is produced, which alters the purity of refraction.

All conventional ray optics may be revisited under the light of the unusual and exotic effects achieved with LH lenses [12, 13]. For instance, Fig 2.11 depicts the reversal of the convergence and divergence effects of convex (parabolic) and concave (hyperbolic) lenses, respectively, when the conventional RH lens is replaced by a LH lens [5]. The diverging effect of the convex lens and the converging effect of the converging lens are readily understood from simply ray optics based on Snell's law [Eq. (2.56)]. In practice, curved interface (e.g., parabolic or hyperbolic) with a LH MTM may be obtained only in a staircase fashion due to the structural nature of the MTM. However, if $p/\lambda_g \ll 1$, the scattering effects of this interface "quantization" are negligible.

Among the potential benefits of replacing conventional (RH) lenses by LH lenses, we may mention the following example [20]. The focal length in a thin lens is given by [11]

$$f = \frac{R}{|n-1|}, \tag{2.67}$$

where R is the radius of curvature of the surface of the lens. From this formula, it appears that, for a given R, a lens with an index of $n = -1$ would have the

[22] As pointed out in Section 1.5, the rule of thumb $p < \lambda_g/4$ ensures predominance of refracted effects over diffraction/scattering effects, but at $p \approx \lambda_g/4$ there is nevertheless some amount of spurious scattering. Scattering may be considered negligible at frequencies where $p < \lambda_g/10, \lambda_g/15$.

same focal length as a lens of index $n = +3$. By the same reasoning, we see, by comparing a RH lens and a LH lens with same index magnitude, that the LH lens would have a smaller focal length and would therefore be more compact. Another observation from the focal length formula is that a RH lens of $n = +1$ would not focus electromagnetic waves (since $f = \infty$), whereas a LH lens with the same density, $n = -1$, would, with a focal length of $f = R/2$.

2.11 SUBWAVELENGTH DIFFRACTION

In [19], Pendry suggested that the subwavelength diffraction limit encountered in conventional lenses could be overcome by Veselago's LH "flat lens" (Fig 2.8) with $\varepsilon_r = \mu_r = -1$, and therefore $n = -1$. In this section, we reproduce the argument of [19], explain this phenomenon in the perspective of surface plasmons, and also point out the practical limitations of such a subwavelength lens.

Consider an infinitesimal dipole of frequency ω in front of a lens with axis z, as illustrated in Fig 2.12. The electric field produced by this source may be expressed in term of the 2D Fourier expansion

$$\overline{\mathsf{E}}(r, t) = \overline{E}(\overline{r})e^{j\omega t} = \sum_m \sum_{k_x, k_y} \widetilde{\overline{E}}_m(k_x, k_y)e^{-j(k_x x + k_y y + k_z z - \omega t)}, \tag{2.68}$$

with, from the wave equation,

$$k_{iz} = p_i - jq_i = \begin{cases} \sqrt{k_i^2 - (k_x^2 + k_y^2)} & \text{if } k_x^2 + k_y^2 = k_\rho^2 < k_i^2, \\ -j\sqrt{(k_x^2 + k_y^2) - k_i^2} & \text{if } k_x^2 + k_y^2 = k_\rho^2 > k_i^2, \end{cases} \tag{2.69a}$$

where k_i is the wave number in the medium i ($i = 1, 2$; 1: air, 2: lens)

$$k_i = (\omega/c)\sqrt{\varepsilon_{ri}\mu_{ri}}. \tag{2.70}$$

All of the information on the image (included in a $x - y$ plane) to be focused by the lens are included in their spectral components k_x and k_y, also referred to as *spatial frequencies*. By Fourier transform between the spatial (x, y) to the spectral (k_x, k_y) domains of the image, the meaning of the spatial frequencies k_ρ, associated with the image wavelength $\lambda_\rho = 2\pi/k_\rho$, is readily understood. Small k_ρs correspond to bulk features of the image, while large k_ρs correspond to detailed features of the image. The information on the image is carried to the lens in the air region by a wave propagating along z. Considering the z dependence of this wave, $e^{-jk_z z}$ ($k_z = k_{1z}$, air region), we see from Eq. (2.69) that, if $k_\rho < k_0$ or equivalently $\lambda_\rho > \lambda_0$, then k_z is real; therefore, the wave really propagates along z and the contents of the image are transmitted to the lens, which accomplishes focusing. This is the situation illustrated in Fig 2.12(a). In contrast,

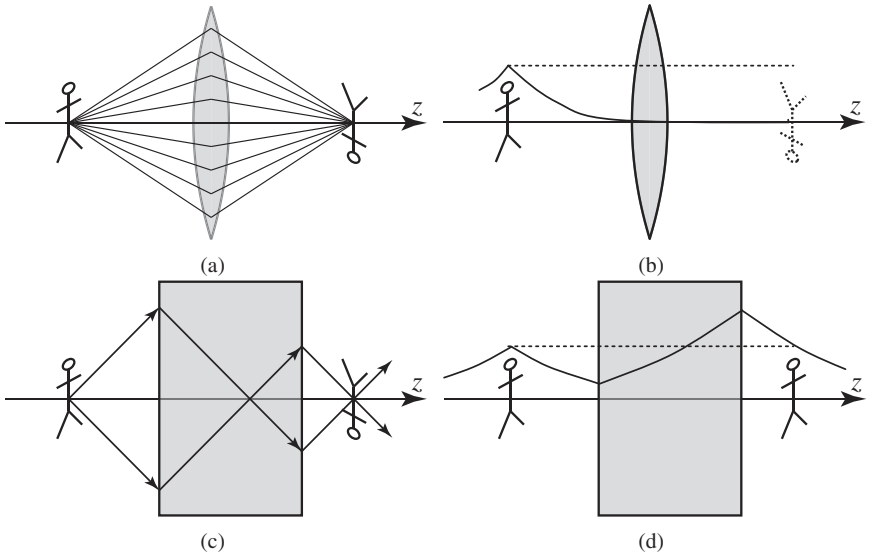

Fig. 2.12. Imaging subwavelength limit and subwavelength diffraction (the lenses are assumed to be in air). Reproduced from [20]. (a) Conventional (RH) lens for incident propagating waves, corresponding to low-spatial frequency components (bulk features) of the source $k_\rho < k_0$: focusing occurs. (b) Conventional (RH) focusing lens for incident evanescent waves, corresponding to high-spatial frequency components (details) of the source $k_\rho > k_0$: source information does not reach the source. (c) LH slab with $\varepsilon_r = \mu_r = -1$ for incident propagating waves, corresponding to low-spatial frequency components: focusing occurs. (d) LH slab with $\varepsilon_r = \mu_r = -1$ for incident evanescent waves, corresponding to high-spatial frequency components: information reaches the source due to energy enhancement related to surface plasmon resonance at each of the two interfaces.

if $k_\rho > k_0$ or $\lambda_\rho < \lambda_0$, k_z is imaginary; therefore, the wave is evanescent along z and the contents of the image either do not reach the lens or are strongly attenuated when reaching the location of focus. This is the situation illustrated in Fig 2.12(b). These considerations show that a conventional lens operates lowpass filter in terms of spatial frequencies of the image at the input of the system: bulk features of the image, transported by propagating components of the wave, are well transmitted, whereas details, included in the evanescent components of the wave, are lost in the transmission process. The spatial frequency limit is given as $k_\rho = k_0$, or equivalently $\lambda_\rho = \lambda_0$. This is the fundamental *diffraction limit* of conventional optics, which may be formulated as follows: the resolution Δ of an optical system is limited by the wavelength of the wave transporting the image

$$\Delta \approx \lambda_{\rho,min} = \frac{2\pi}{k_{\rho,max}} = \frac{2\pi}{k_0} = \frac{2\pi c}{\omega} = \lambda_0. \tag{2.71}$$

Let us now show how Pendry demonstrated that this diffraction limit could, theoretically, be overcome in a LH slab with ε_r and $\mu_r = -1$. In this case,

$|k_{1z}| = |k_{2z}|$, and we have from Eq. (2.69),[23] where the subscripts 1 and 2 refer to air and to the LH medium of the slab, respectively,

$$k_{2z} = p_2 = -k_{1z} = -p_1 \quad \text{if} \quad k_{1z}, k_{2z} \in \mathbb{R} \quad \text{(propagating wave)}, \tag{2.72a}$$

$$k_{2z} = p_2 = +k_{1z} = p_1 \quad \text{if} \quad k_{1z}, k_{2z} \in \mathbb{I} \quad \text{(evanescent wave)}, \tag{2.72b}$$

where the first relation accounts for NRI of the wave when it is propagating and the second relation ensures exponential decay of the wave when it is evanescent ($\mathbb{R}$ stands for purely real and $\mathbb{I}$ for purely imaginary).

The Fresnel coefficients from medium 1 to medium 2 and from medium 2 to medium 1 are given by Eq. (2.59). Let us for instance consider the case of perpendicular polarization. We have

$$R_{\parallel}^{1\to 2} = \frac{\mu_{r2}k_{2z} - \mu_{r1}k_{1z}}{\mu_{r2}k_{2z} + \mu_{r1}k_{1z}} = r, \quad T_{\parallel}^{1\to 2} = \frac{2\mu_{r2}k_{1z}}{\mu_{r2}k_{2z} + \mu_{r1}k_{1z}} = t, \tag{2.73a}$$

$$R_{\parallel}^{2\to 1} = \frac{\mu_{r1}k_{1z} - \mu_{r2}k_{2z}}{\mu_{r1}k_{1z} + \mu_{r2}k_{2z}} = r', \quad T_{\parallel}^{2\to 1} = \frac{2\mu_{r1}k_{2z}}{\mu_{r1}k_{1z} + \mu_{r2}k_{2z}} = t'. \tag{2.73b}$$

It is then possible to compute the total transmission and reflection coefficients by summing the *multiple reflections* events

$$T_{\parallel} = tt'e^{-jk_{2z}d} + tt'r'^2e^{-j3k_{2z}d} + tt'r'^4e^{-j5k_{2z}d} + \ldots = \frac{tt'e^{-jk_{2z}d}}{1 - r'^2e^{-j2k_{2z}d}}, \tag{2.74a}$$

$$R_{\parallel} = r + tt'r'e^{-jk_{2z}d} + tt'r'^3e^{-j3k_{2z}d} + \ldots = r + \frac{tt'r'e^{-j2k_{2z}d}}{1 - r'^2e^{-j2k_{2z}d}}. \tag{2.74b}$$

Let us now consider the overall transmission coefficient. By inserting Eq. (2.73) into Eq. (2.74a), we obtain with Eq. (2.72b) in the case of an *evanescent wave*

$$T_{\parallel}^{\text{evan.(LH)}} = \lim_{\substack{\mu_{r1}\to+1 \\ \mu_{r2}\to-1}} \frac{tt'e^{-jk_{2z}d}}{1 - r'^2e^{-j2k_{2z}d}}$$

$$= \lim_{\substack{\mu_{r1}\to+1 \\ \mu_{r2}\to-1}} \frac{2\mu_{r2}k_{1z}}{\mu_{r2}k_{2z} + \mu_{r1}k_{1z}} \frac{2\mu_{r1}k_{2z}}{\mu_{r1}k_{1z} + \mu_{r2}k_{2z}} \frac{e^{-jk_{2z}d}}{1 - \left(\frac{\mu_{r1}k_{1z} - \mu_{r2}k_{2z}}{\mu_{r1}k_{1z} + \mu_{r2}k_{2z}}\right)^2 e^{-j2k_{2z}d}}$$

$$= \frac{-2k_{1z}}{-k_{2z} + k_{1z}} \frac{2k_{2z}}{k_{1z} - k_{2z}} \frac{e^{-jk_{2z}d}}{1 - \left(\frac{k_{1z} + k_{2z}}{k_{1z} - k_{2z}}\right)^2 e^{-j2k_{2z}d}}$$

[23] Again, we consider a loss-less slab for simplicity.

$$= \frac{-4k_{1z}k_{2z}}{(k_{1z}-k_{2z})^2} \frac{e^{-jk_{2z}d}}{1-\left(\frac{k_{1z}+k_{2z}}{k_{1z}-k_{2z}}\right)^2 e^{-j2k_{2z}d}}$$

$$\overset{(k_{2z}=k_{1z}=k_z)}{=} e^{+jk_zd} \overset{(k_z=-ja)}{=} e^{+qd} \quad (q \in \mathbb{R}, q > 0). \tag{2.75}$$

This result shows that *an evanescent wave is enhanced by a LH slab*, as illustrated in Fig 2.12(d).[24] This enhancement phenomenon is simply due to the excitation of a resonance mode of each of the interface, called a *surface plasmon*.[25] Thus, subwavelength details ($\lambda_\rho < \Delta \approx \lambda_0$) of the image can be focused by the LH slab. Bulk features of the image are clearly transmitted, as already shown in Section 2.7 and illustrated in Fig 2.12(c).

For the sake of completeness, let us consider what happens if the evanescent wave would be incident upon RH slab (for which we have $k_{2z} = k_{1z} = -jq$ for exponential decay at infinity)

$$T_{\parallel}^{\text{evan.(RH)}} = \lim_{\substack{\mu_{r1}\to+1 \\ \mu_{r2}\to+1}} \frac{tt'e^{-jk_{2z}d}}{1-r'^2e^{-j2k_{2z}d}}$$

$$= \lim_{\substack{\mu_{r1}\to+1 \\ \mu_{r2}\to+1}} \frac{2\mu_{r2}k_{1z}}{\mu_{r2}k_{2z}+\mu_{r1}k_{1z}} \frac{2\mu_{r1}k_{2z}}{\mu_{r1}k_{1z}+\mu_{r2}k_{2z}} \frac{e^{-jk_{2z}d}}{1-\left(\frac{\mu_{r1}k_{1z}-\mu_{r2}k_{2z}}{\mu_{r1}k_{1z}+\mu_{r2}k_{2z}}\right)^2 e^{-j2k_{2z}d}}$$

$$= \frac{2k_{1z}}{k_{2z}+k_{1z}} \frac{2k_{2z}}{k_{1z}+k_{2z}} \frac{e^{-jk_{2z}d}}{1-\left(\frac{k_{1z}-k_{2z}}{k_{1z}+k_{2z}}\right)^2 e^{-j2k_{2z}d}}$$

$$= \frac{4k_{1z}k_{2z}}{(k_{1z}+k_{2z})^2} \frac{e^{-jk_{2z}d}}{1-\left(\frac{k_{1z}-k_{2z}}{k_{1z}+k_{2z}}\right)^2 e^{-j2k_{2z}d}}$$

$$\overset{(k_{2z}=k_{1z}=k_z)}{=} e^{-jk_zd} \overset{(k_z=-jq)}{=} e^{-qd} \quad (q \in \mathbb{R}, q > 0) \tag{2.76}$$

We see that, in this case, the typically expected exponential decay is observed.

Subwavelength diffraction with a $\varepsilon_r = \mu_r = -1$ LH slab suggests the theoretical idea of infinite resolution focusing. In practice, the severe constraint that the lens must have exactly $\varepsilon_r = \mu_r = -1$ limits this phenomenon. If this condition is not satisfied, spherical aberration (Section 2.7) and mismatch losses (Section 2.8)

[24]The same conclusion is straightforwardly obtained in the case of perpendicular polarization, where the fact that $\mu_{r1} \to +1$ $\varepsilon_{r2} \to -1$ is used in the derivations.

[25]MTM surface plasmons are illustrated by full-wave simulated fields in Section 4.4.4 and discussed in the perspective of potential novel applications in Section 4.5.1.

occur and ruin the theoretical interest of the lens. Such limitations are discussed in several papers (e.g., [21, 22]). Subwavelength focusing was demonstrated experimentally in the SRR-TW structure by Lagarkov et al. in [22] and in a 2D planar transmission line structure by Grbic et al. in [23]. In [24], regeneration of evanescent waves from a silver ($\varepsilon_r \approx -1$) superlens was demonstrated experimentally.[26] Note that performance is predicted from alternating parallel sided layers of $n = -1$ and $n = +1$ material, which also acts as a "lens" [25, 26].

REFERENCES

1. M. D. Pozar. *Microwave Engineering,* Third Edition, John Wiley & Sons, 2004.
2. L. Brillouin. *Wave Propagation and Group Velocity,* Academic Press, 1960.
3. E. M. Lifshitz, L. D. Landau, and L. P. Pitaevskii. *Electrodynamics of Continuous Media: Volume 8,* Second Edition, Butterworth-Heinemann, 1984.
4. J. D. Kraus and R. J. Marhefka. *Antennas,* Third Edition, McGraw Hill, 2001.
5. V. Veselago. "The electrodynamics of substances with simultaneously negative values of ε and μ," *Soviet Physics Uspekhi,* vol. 10, no. 4, pp. 509–514, Jan.-Feb. 1968.
6. R. J. Doviak, D. S. Zrnic, and R. J. Doviak. *Doppler Radar and Weather Observations,* Second Edition, Academic Press, 1993.
7. J. A. Kong. *Electromagnetic Wave Theory,* Second Edition, John Wiley & Sons, 1990.
8. C. Caloz and T. Itoh. "Array factor approach of leaky-wave antennas and application to 1D/2D composite right/left-handed (CRLH) structures," *IEEE Microwave Wireless Compon. Lett.,* vol. 14, no. 6, pp. 274–276, June 2004.
9. J. L, T. M. Grzegorczyk, Y. Zhang, J. Pacheo, B.-I. Wu, J. A. Kong, and M. Chen. "Čerenkov radiation in materials with negative permittivity and permeability," *Optics Express,* vol. 11, no. 7, pp. 723–734, April 2003.
10. A. Ishimaru. *Electromagnetic Wave Propagation, Radiation, and Scattering*, Prentice Hall, 1991.
11. M. Born and E. Wolf. *Principles of Optics,* Seventh Edition, Cambridge University Press, 2002.
12. D. Schurig and D. R. Smith. "Universal description of spherical aberration free lenses composed of positive or negative index media," *Phys. Rev. E,* eprint physics/0307088, 2003.
13. D. Schurig and D. R. Smith. "Negative index lens aberrations," *Phys. Rev. E,* eprint physics/0403147 v1, 2003.
14. H. K. V. Lotsch. "Beam displacement at total reflection: the Goos-Hänchen effect," *I. Optik,* vol. 32, pp. 116–137, 1970.
15. F. Goos and H. Hänchen. "Ein neuer und fundamentaler Versuch zur Totalreflexion," *Ann. Phys. Lpz,* vol. 1, pp. 333–346, 1947.

[26]A slab with only $\varepsilon_r = -1$ represents a simplification of the "perfect lens" (p-polarized fields), which is possible when all length scales are much smaller than the wavelength of light (quasistatic limit) [19]. Subwavelength resolution is then possible in principle for example with thin silver films, which exhibit a permittivity equal to -1 in the visible region of the spectrum, although losses still represent a severe limitations in this approach.

16. A. Lakhtakia. "Positive and negative Goos-Hänchen shifts and negative phase-velocity mediums (alias left-handed materials)," *Int. J. Electron. Commun.,* vol. 58, no. 3, pp. 229–231, 2004.
17. P. R. Berman. "Goos-Hänchen shift in negatively refractive media," *Phys. Rev. E,* vol. 66, pp. 067603:1–3, 2002.
18. I. V. Shadrivov, R. W. Ziolkowski, A. A. Zharov, and Y. S. Kivshar. "Excitation of guided waves in layered structures with negative refraction," *Optics Express,* vol. 13, no. 2, pp. 481–492, Jan. 2003.
19. J. B. Pendry. "Negative refraction makes a perfect lens," *Phys. Rev. Lett.,* vol. 85, no. 18, pp. 3966–3969, Oct. 2000.
20. D. R. Smith and J. B. Pendry. "Reversing light: negative refraction," *Physics Today,* pp. 1-8, Dec. 2003.
21. D. R. Smith, D. Schurig, M. Rosenbluth, and S. Schultz. "Limitations on subdiffraction imaging with a negative refractive index slab," *App. Phys. Lett.,* vol. 82, no. 10, pp. 1506–1508, March 2003.
22. A. N. Lagarkov and V. N. Kissel. "Near-perfect imaging in a focusing system based ona left-handed-material plate," *Phys. Rev. Lett.,* vol. 92, no. 7, pp. 077401:1–4, Feb. 2004.
23. A. Grbic and G. Eleftheriades. "Overcoming the diffraction limit with a planar left-handed transmission-line lens," *Phys. Rev. Lett.,* vol. 92, no. 11, pp. 117403:1–4, March 2004.
24. N. Fang, Z. Liu, T.-J. Yen, and X. Zhang. "Regenerating evanescent waves from a silver superlens," *Optics Express,* vol. 11, no. 7, pp. 682–687, March 2004.
25. E. Shamonina, V. A. Kalinin, K. H. Ringhofer, and L. Solymar. "Imaging compression and Poynting vector streamlines for negative permittivity materials," *Electron. Lett.,* vol. 37, no. 20, pp. 1243–1244, Sept. 2001.
26. S. .A. Ramakrishna, J. B. Pendry, M. C. K. Wiltshire, and W. J. Stewart. "Imaging the near field," *J. Mod. Opt.,* vol. 50, pp. 1419–1430, 2003.